

## Langmuir circulation within the oceanic mixed layer

ROBERT A. WELLER\* and JAMES F. PRICE\*

(Received 15 June 1987; in revised form 23 November 1987; accepted 27 November 1987)

**Abstract**—The three-dimensional flow in the mixed layer associated with Langmuir circulation was studied with a new instrument capable of directly measuring the three components of velocity. Regions of convergent surface flow were located with surface drifters. In these regions the downward vertical and downwind horizontal components of the flow were comparable in size and, at times, in excess of  $20 \text{ cm s}^{-1}$ . This downwind, downwelling flow was jet-like in structure, with the maximum velocity located below the surface. Away from the downwelling regions and in the lower half of the mixed layer below the convergence zones, the flow associated with the Langmuir cells was an order of magnitude smaller and not well resolved in these experiments. On some occasions, when Langmuir cells appeared suddenly, they were able to mix the weak near-surface stratification that had formed in response to diurnal heating. They could also maintain large shears in the well-mixed fluid near the surface. They did not, however, penetrate with strength to the base of relict mixed layers observed during summer-like conditions or to the base of deeper, more isothermal, mixed layers observed during stormy conditions.

### 1. INTRODUCTION

LANGMUIR (1938) observed long, narrow rows of seaweed on the sea surface aligned nearly parallel to the wind in the open Atlantic. Intrigued by the notion that the pattern of the seaweed indicated the presence of organized, three-dimensional flow within the near-surface layer of the ocean, LANGMUIR (1938) carried out a series of flow visualization experiments in Lake George. These experiments confirmed the presence of counter-rotating vortices whose axes were aligned nearly parallel to the wind; flotsam and surface films formed rows when swept into the convergent regions between adjacent vortices. These vortices are now called Langmuir cells, and the flow associated with these somewhat regularly spaced cells is called Langmuir circulation.

Such relatively large, organized, three-dimensional flows should play a significant role in the transport of heat, momentum and other properties down from the air–sea interface into the interior. They also should affect the distribution of plants and animals, both in the near-surface region (SUNDBY, 1983) and on the surface (FALLER and AUER, 1987), and the air–sea exchange of gases (FALLER and PERINI, 1983) and other matter. In addition, they probably complicate attempts to sample mean properties of the surface layer with Lagrangian drifters.

A number of investigations, including theoretical, laboratory and field studies, have tried to determine the role of Langmuir circulation in various upper ocean processes; LEIBOVICH (1983) and POLLARD (1977) provide good reviews of the efforts completed prior to 1983. However, in spite of these studies it had remained unclear whether or not

---

\* Woods Hole Oceanographic Institution, Woods Hole, MA 02543, U.S.A.

Langmuir circulation was a significant mechanism for mixing and vertical redistribution in the mixed layer and thus whether or not it played a significant role in upper ocean dynamics. More widely accepted was the notion that small scale turbulence was the predominant mechanism for mixing and vertical transfer. In part, the uncertainty about the role of Langmuir circulation was due to the relatively small size of the downward vertical velocities, approximately  $5 \text{ cm s}^{-1}$  and less, reported in the literature. Also, because most measurements had been made at or near the surface, the depth and strength of penetration and the vertical structure of Langmuir cells were not well known.

Our interest stems from a 1980 field study of mixed layer dynamics (PRICE *et al.* 1986) that led us to consider the possibility that Langmuir cells were present. In that experiment the vertical shear of horizontal velocity, averaged over 5 min intervals, was observed to be small in the mixed layer. Fresh inputs of momentum from changes in the direction and/or magnitude of the wind stress were distributed rapidly (on time scales shorter than or comparable to the 30 min spacing between successive profiles of horizontal velocity and temperature) over the homogeneous region of the mixed layer. The observed lack of wind-driven shear suggested the existence, at least at some times, of a mechanism more efficient at vertical transfer than small scale turbulence, and thus supported the hypothesis that Langmuir circulation was present. However, because the vertical component of velocity had not been measured and no other attempt had been made during this experiment to look for evidence of large scale, organized, three-dimensional flow within the mixed layer, it was not possible to test this hypothesis.

In the next field experiment we deployed a new current meter designed to measure the three components of velocity and included a measurement program designed specifically to look for evidence of three-dimensional flows and, if possible, to characterize their strength and structure. During this field study three cruises were conducted on the Research Platform *Flip*. On the first cruise the new instrumentation proved capable of observing three-dimensional flow within the mixed layer, and evidence of strong Langmuir cells was found (WELLER *et al.* 1985). In the second and third cruises our measurements were made simultaneously with Doppler sonar measurements by R. Pinkel of the Scripps Institution of Oceanography. The Doppler sonar, with a range of up to 1400 m, also observed the Langmuir circulation, confirming the representativeness of the point measurements made by our mechanical current meters and provided additional information about the spatial extent and temporal persistence of the Langmuir cells (SMITH *et al.*, 1987).

The purposes of this paper are to make a detailed report of the characteristics of the Langmuir circulation observed during the three cruises and to present evidence of how Langmuir circulation modifies the structure of the mixed layer. The specifics of the instrumentation and measurement strategy are summarized; then the observations of the Langmuir circulation are presented. Evidence of modification of the structure of the mixed layer by the Langmuir circulation is shown next. In addition, the observations are compared with the previously reported characteristics of Langmuir circulation.

## 2. INSTRUMENTATION AND DATA COLLECTION

All three cruises were conducted on the Research Platform *Flip* off the coast of California (Fig. 1). Cruises 1 (on station from 11 to 17 December 1982) and 2 (on station from 13 to 19 May 1983), each about 1 week long, were carried out 200 and 400 km west-

## (a) FLIP DRIFT TRACKS – DEC 82, MAY 83, OCT 83

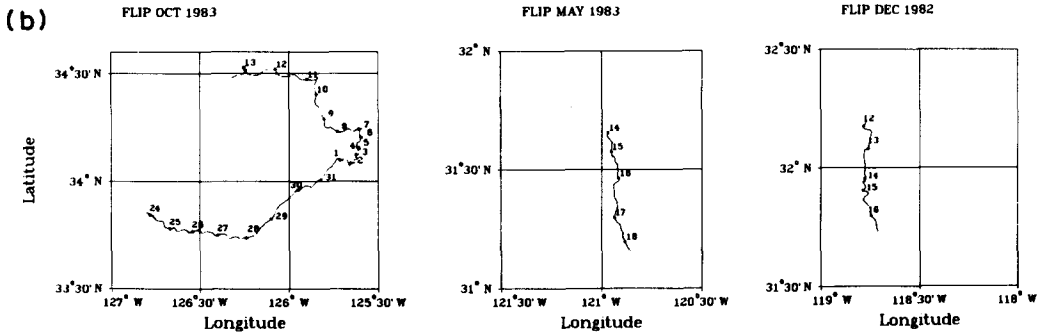
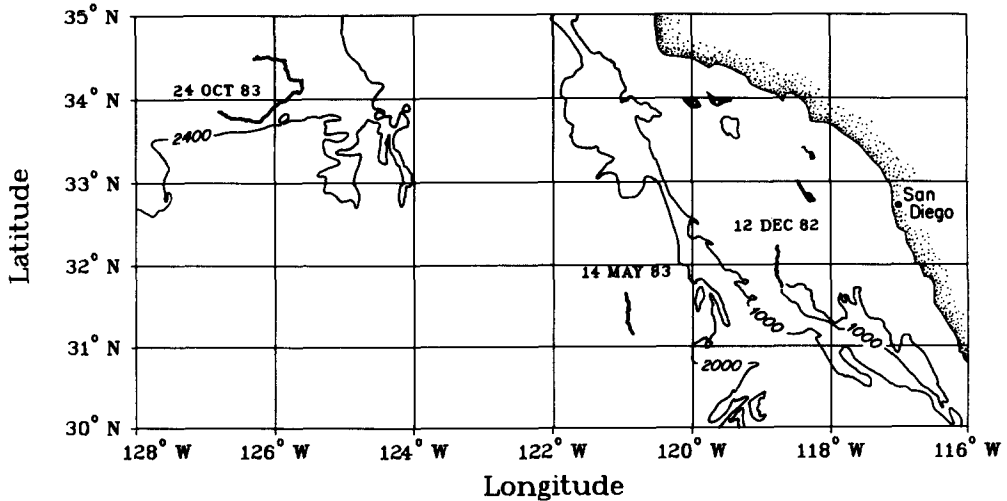


Fig. 1. The locations of the three cruises on the R.P. *Flip* (a) and *Flip*'s drift track during each cruise (b). Day tics are labeled with days of the month in (b).

southwest of San Diego, respectively. The third cruise, conducted as part of the Mixed Layer Dynamics Experiment (MILDEX), was longer (on station from 23 October to 15 November 1983) and further offshore, some 850 km west-northwest of San Diego and roughly 500 km west of Pt. Conception.

During each cruise Vector Measuring Current Meters (VMCMs) (WELLER and DAVIS, 1980) were deployed from booms attached to *Flip* (Fig. 2). Some were stationed at fixed depths, and an automated winch was used to cycle up to four other VMCMs vertically every half hour over a depth range of up to approximately 10–165 m. This method of collecting both time series at fixed depths and vertical profiles of temperature and horizontal velocity relative to *Flip* has been described by WELLER (1981) and PRICE *et al.*

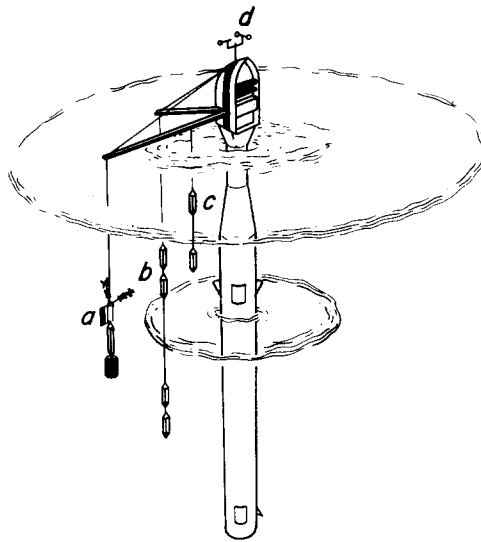


Fig. 2. A sketch of R.P. *Flip* showing the location of the instrumentation. The Real Time Profiler (a) was deployed off the end of a 15 m boom on the port side. Automatically profiling VCMCs (b) were deployed from a 10 m boom angled slightly forward off the port side. Fixed level VCMCs (c) and the second RTP were deployed part way out the 15 m boom. Meteorological measurements were made from the mast (d).

(1986). The VCMCs recorded vector-averaged horizontal velocity components, temperature (from an external sensor with a response time of approximately 6 s), and pressure every minute.

Meteorological data, including wind speed and direction, air and sea temperatures, barometric pressure, solar radiation and relative humidity, were recorded every 7.5 min by a meteorological data logger (a Vector Averaging Wind Recorder or VAWR) mounted on *Flip*'s mast. *Flip*'s position was determined by an Internav LORAN C receiver and recorded every minute. Supplemental manual observations of cloud cover, wet and dry bulb temperatures, wind velocity, and sea state were made every 15 min. In MILDEX, wave heights were also available from two resistance wires deployed from *Flip*'s booms by R. Pinkel.

A new instrument, the Real Time Profiler (RTP) (Fig. 3), was deployed during these cruises with the specific intent of looking for evidence of Langmuir circulation. The RTP, like the VAWR and VCMCs, recorded data internally; unlike those instruments it also provided data via cable for real time display. The RTP was constructed by modifying a Savonius rotor and vane Vector Averaging Current Meter (VACM, manufactured by EG&G Sea Link, Herndon, Virginia). Two VCMC velocity sensors, each with two orthogonal propellers, were mounted at right angles in place of the Savonius rotor, and a large fin was mounted to orient the instrument with respect to the flow. The orientation of the fin was chosen to minimize disturbance of the flow prior to reaching the propeller sensors. Along the top of the fin an external temperature sensor identical to that used with the VCMC and a Seabird conductivity cell were fitted.

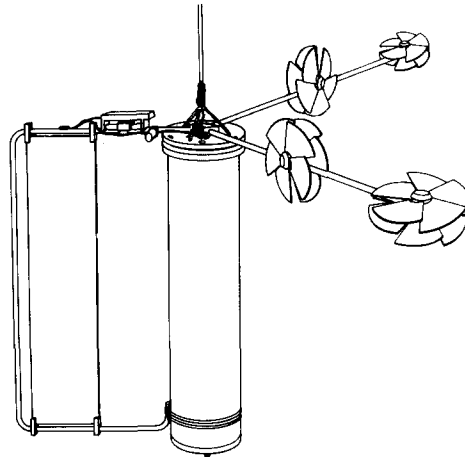


Fig. 3. The Real Time Profiler (RTP). Two dual propeller VMCM sensors mounted at right angles provided measurements of the three orthogonal components of velocity (with two redundant measurements of the vertical component). A Seabird conductivity cell and a temperature sensor are mounted on the top of a frame that supports a fin for orienting the instrument relative to the flow.

The VMCM propeller sensors were used on the RTP because of their accurate cosine response and because of their ability to accurately measure small mean flows in the presence of large oscillatory flows such as those associated with surface waves (WELLER, 1978; BEARDSLEY, 1987). In order to minimize their threshold, the propellers for the RTP were made from plastic with near neutral buoyancy and precision ball bearings were fitted. Each propeller sensor, as in the VMCM, used magnets and a pair of magnetodiodes to permit determination of its direction as well as its rate of revolution; the resolution of these propeller sensors was one count per 8 cm of fluid displacement parallel to its axle. Propeller counts were summed in up-down counters over each sample interval. The four propellers on the two orthogonal VMCM sensors measured two orthogonal components of velocity in the horizontal plane and two redundant values of the vertical component. Taking the performance characteristics of the modified VMCM propeller sensors, the sampling rate, and the noise level provided by the surface wave flow field and the motion of *Flip* into account, the RTP was capable of detecting mean vertical velocities with magnitudes of approximately  $2 \text{ cm s}^{-1}$  and higher if they persisted over one or more sampling intervals.

During each experiment, one RTP, with a VMCM and a fluorometer shackled below, was attached to a winch capable of profiling very slowly ( $15 \text{ m h}^{-1}$ ) and operated manually from the lab under the control of an operator monitoring the real time display of the two observed vertical components, of  $u$  and  $v$ , the east-west and north-south components of velocity computed from the observed horizontal flow, and of temperature, depth, conductivity and tilt. This RTP and associated VMCM were used to collect vertical profiles of varying depth resolution by varying descent/ascent rates and also to collect time series by parking the instruments at selected depths. Depth information from a strain gauge pressure transducer was used to remove vertical motion of the package from vertical velocities computed during profiling. The mass of the instruments shackled below helped minimize tilting of the RTP. The tilt signals were typically small, always

below 2–3°. Without tilt correction, the false vertical velocity,  $(u^2 + v^2)^{1/2} \sin \alpha$ , where  $\alpha$  is the tilt, was at most  $2.5 \text{ cm s}^{-1}$ . Thus, the real time displays of the vertical velocity were only slightly biased. However, while no tilt correction was made for the real time display, data from the RTP were recorded on tape and post-cruise computation of  $u$ ,  $v$  and  $w$  from the propeller counts used both the compass and two axes of tilt information so that the effect of tilt was removed prior to post-cruise analysis.

Sea surface conditions were monitored by several means, and log entries were made of any sightings of surface slicks during RTP operation. In addition, surface drifters were used to monitor the presence, scales and strength of convergent/divergent surface flows. During daylight, used IBM cards were scattered from the upper decks on *Flip*. The time required for the cards to line up and the approximate length of and spacing between the card lines were recorded. The direction of the surface wind was visualized by releasing floating smoke markers (see Fig. 4). At night, the surface was seeded with drifters when the RTP data indicated the presence of vertical flow. In this case, small plastic bags filled with luminescent fluid were used in place of the computer cards to verify that surface convergences coexisted with the downwelling events observed with the RTP. The organization of the drifters, which were widely distributed, into long, narrow lines aligned nearly parallel to the wind provided independent verification of the presence of Langmuir cells and was used to guide and complement data collection with the RTP. If strong vertical flow was observed in the real time display of the RTP data, surface drifters were deployed to verify that alternating regions of convergent and divergent surface flow were present around *Flip* and an attempt was made to correlate the actual crossing of card lines with the real time observation of vertical flow by the RTP. If the RTP failed to find evidence of Langmuir cells, surface drifters were scattered to verify that three-dimensional flow was weak or absent and rule out the possibility of fouling or other malfunction of the propeller sensors.

Details of the data collection efforts and environmental conditions during each of the three cruises are summarized below:

#### *December 1982*

In December 1982, data was collected from 12 to 16 December while *Flip* drifted southward. Relatively calm conditions were encountered (Fig. 5). Surface wave heights were moderate, typically 1–2 m. The southerly winds were moderate, averaging  $8 \text{ m s}^{-1}$  with a peak of  $14 \text{ m s}^{-1}$  on 13 December. After 13 December the winds decreased and became light ( $5 \text{ m s}^{-1}$ ), remaining so under clear, sunny skies until the beginning of 16 December. Three VMCMs and one RTP were deployed. One VMCM was attached to the automated winch, deployed from the end of a 10 m boom, and used to collect half-hourly profiles of temperature and horizontal velocity in the upper 70 m. The second VMCM was deployed at the fixed depth of 2 m from the end of a 15 m boom, from which the RTP was also deployed. The third VMCM was shackled below the RTP. The mixed layer was approximately 45 m deep for the duration of the experiment, and the flow in the upper 70 m relative to *Flip* did not exceed  $20 \text{ cm s}^{-1}$ .

#### *May 1983*

In May 1983 *Flip* was towed further offshore and again drifted southward. Data were collected with a VAWR mounted in *Flip*'s mast, three VMCMs, and one RTP, all deployed as in December 1982. The winds were relatively steady, varying between 5 and

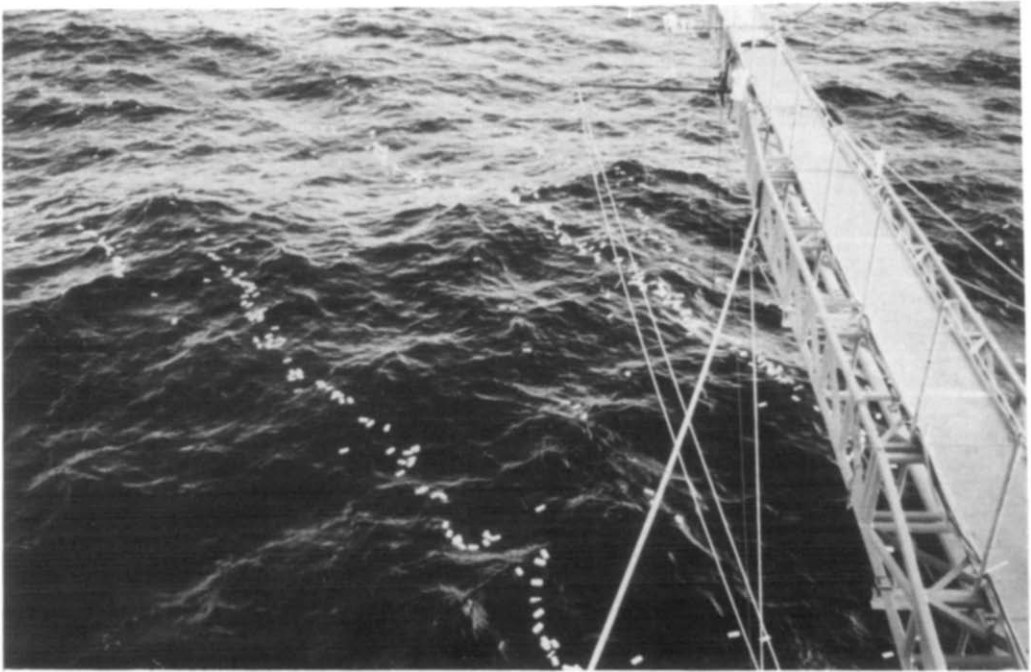


**Fig. 4a.**

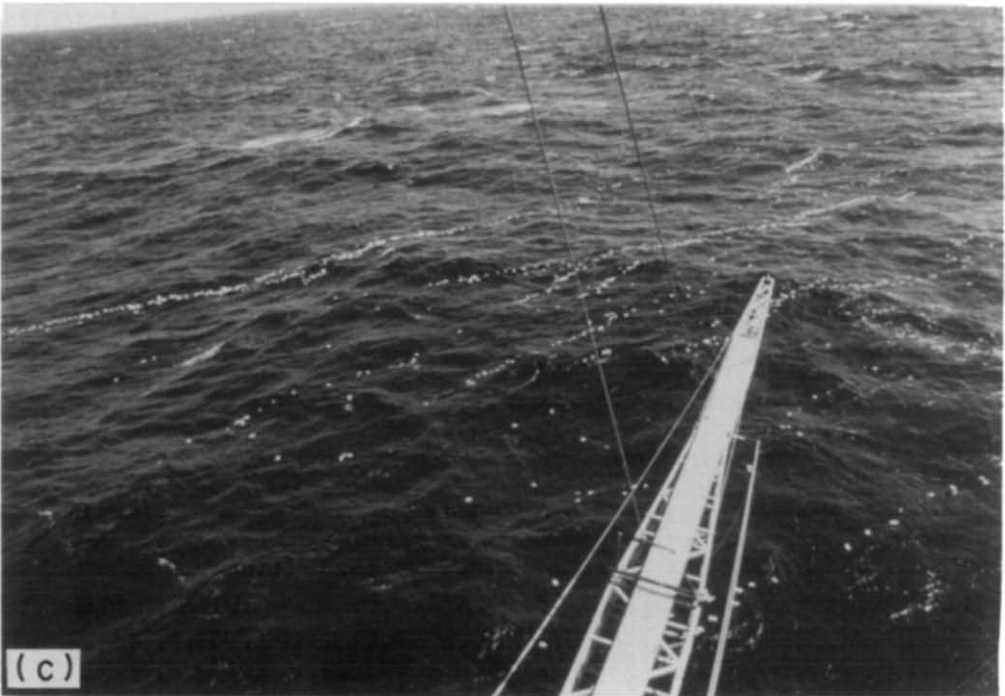


**Fig. 4. Photographs of computer cards on the sea surface. In (a) instruments suspended beneath the booms are moving through the regions of convergent flow marked by lines of computer cards, (b) and (c) show computer cards on other days. The smoke plume results from a floating smoke marker.**

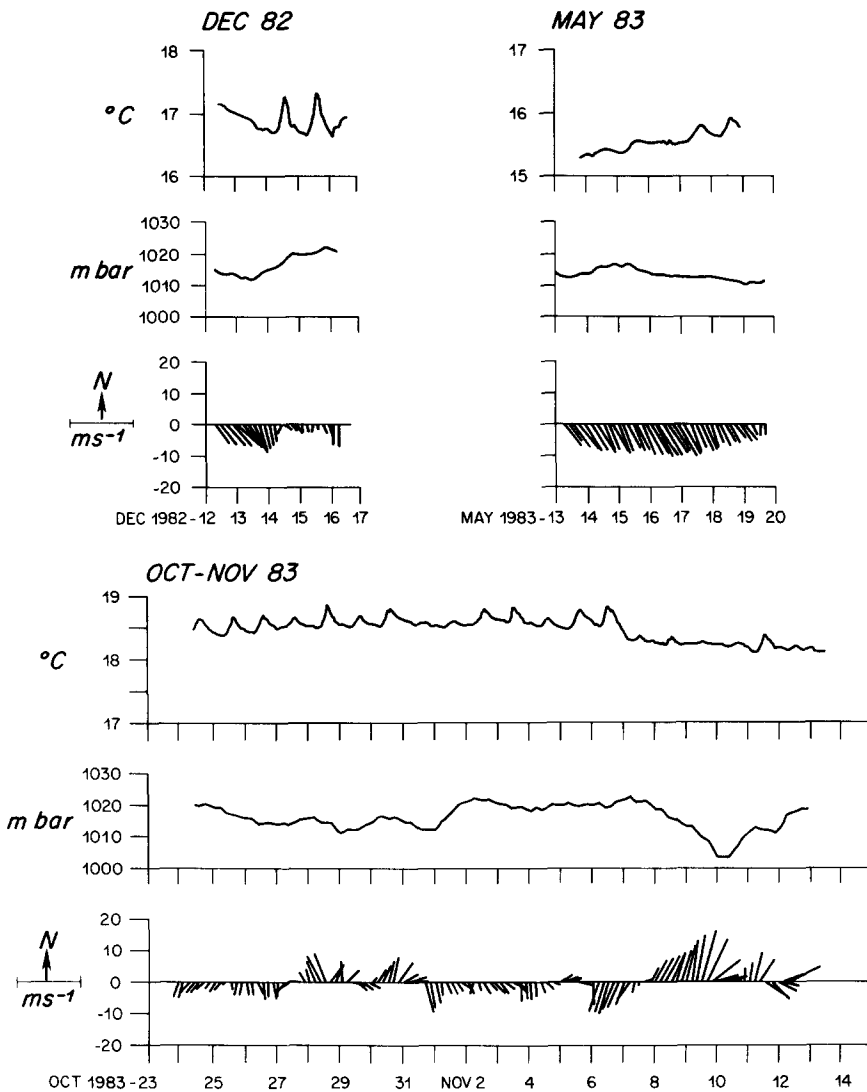


Fig. 5. Sea surface temperature and meteorological conditions during the three cruises. For each cruise, time series of sea surface temperature, barometric pressure, and 4-h average wind velocity are plotted.

$12 \text{ m s}^{-1}$ , and toward the south-southeast (Fig. 5). Two to three meter waves were observed. The weather was clear on 16 May and on most of 18 May, and cloudy on 17 May and late on 19 May. The depth of the mixed layer was 60–70 m, and the flow relative to *Flip* was typically  $10 \text{ cm s}^{-1}$  toward the southwest.

#### October–November 1983, MILDEX

During the third cruise *Flip* drifted counter-clockwise around part of a loop centered near  $34^{\circ}\text{N}$ ,  $126^{\circ}\text{W}$ . One VAWR, eight VMCMs and two RTPs were deployed. Three of

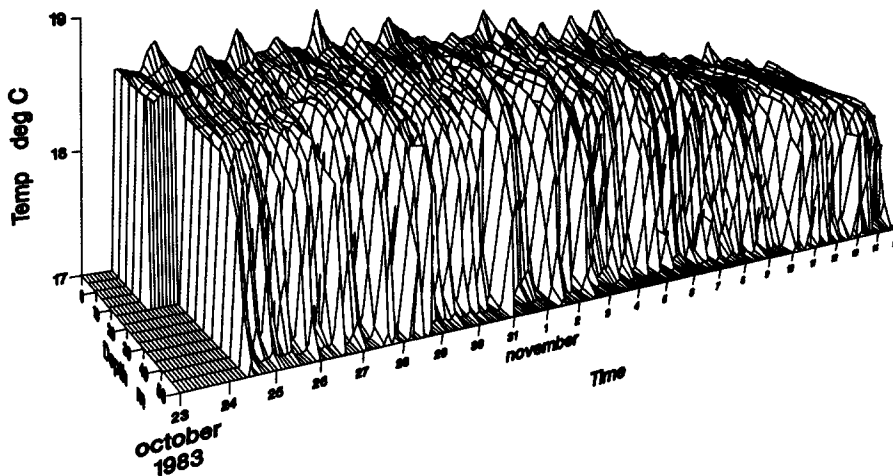


Fig. 6. Temperature in the upper 60 m as a function of depth and time during the the third cruise (MILDEX). Early in the experiment, diurnal variability was evident in the upper 10–15 m, and the 40–50 m deep mixed layer warmed slightly. After 6 November, wind forcing was greater, and the mixed layer was more homogeneous, cooler and slightly deeper.

the eight VMCMs were stationed for the duration of the experiment at the fixed levels of 2, 6.5 and 12 m. Four VMCMs were mounted initially as two pairs of two instruments on the winch that cycled automatically every hour. Within each pair, the instruments were separated by 4.5 m; the two pairs were separated by 70 m. After the drive shaft on that winch sheared twice on 2 November, these instruments were recovered and redeployed at the fixed depths of 20, 35, 50 and 65 m. The eighth VMCM was shackled below the first RTP, which was deployed from near the end of the long boom as in December and May. A second RTP was deployed at a fixed depth of 20 m from a point approximately 10 m out along the same boom; this instrument recorded data internally without output to the lab.

Greater range and variability in the meteorological forcing were encountered during MILDEX (Fig. 5). From the beginning of the experiment until 6 November the winds were light to moderate ( $5\text{--}10\text{ m s}^{-1}$ ) and the skies mostly clear; as a result, strong diurnal variability was observed in the near-surface temperature field (Fig. 6). Stronger wind forcing, up to  $18\text{ m s}^{-1}$ , characterized the weather on and after 6 November, as a series of storms passed through. Together with greater cloud cover, this stronger wind forcing reduced the diurnal variability and led to a more uniform mixed layer of approximately 50 m depth. Flow relative to *Flip* had a magnitude of typically  $15\text{ m s}^{-1}$ . The wind waves had peak amplitudes of 1–2 m in the light conditions during the first half of the experiment, growing to 3–6 m during the storms. Towards the end of the experiment, swells in excess of 10 m generated by gales in the North Pacific were encountered.

### 3. OBSERVATIONS OF LANGMUIR CIRCULATION

The RTP on the manually controlled winch was used to search for evidence of three-dimensional flow. Together with the observations of the surface drifters, the results of

the RTP measurement program provided the best overview or census of the occurrence, strength and characteristics of the observed flow. These observations are presented first. The data from the internally recording VMCMs are then used to illustrate further the characteristics of the flow associated with Langmuir circulation.

### *Real Time Profiler observations*

During the December 1982 cruise the most successful strategy for observing significant, persistent vertical flow in real time was to hold the RTP at a fixed depth in the mixed layer. When profiling, velocity signals changed rather rapidly and were difficult to interpret; but with the RTP held at a fixed depth, downwelling signals that persisted over many surface wave periods were detected in the raw RTP time series. It was possible to correlate the occurrence of many of these downwelling events with the passage of *Flip* through lines of computer cards. Similar records of downwelling events were collected in May 1983 and in MILDEX (Fig. 7). The observed three-dimensional flows were roughly consistent with previous conceptualizations of Langmuir circulation by POLLARD (1977) and others (Fig. 8); and, as a result, the three-dimensional flow shown in Figs 7 and 8 and similar flow observed during these cruises will be referred to as Langmuir circulation. No evidence for other patterns or types of three-dimensional flow in the mixed layer was found, and no evidence of significant vertical velocities was ever found when the RTP was parked at or below the base of the mixed layer.

The strongest downwelling was observed at depths below the surface and above mid-depth in the mixed layer. The strength of the three-dimensional flow also showed considerable temporal variability. A series of strong downwelling events occurring roughly every 10 min for an hour could be followed by an hour with no discernable vertical velocity signal. An attempt was made to assess both the temporal variability and the vertical extent of the vertical flow associated with the Langmuir cells by repositioning the RTP at various depths within the mixed layer and collecting short (typically 30–120 min in length) time series of  $u$ ,  $v$  and  $w$  at each depth. These observations are summarized in Figs 9 and 10. In general, downward flow was observed as relatively well-defined events with amplitudes ranging up to almost  $30 \text{ cm s}^{-1}$ , or an order of magnitude

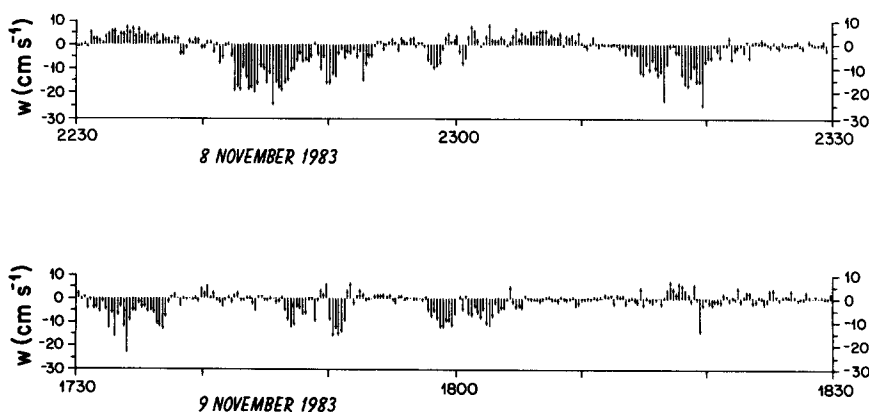


Fig. 7. Raw, original sampling rate (every 14 s) vertical velocity data collected with the RTP during MILDEX. Two, 1 h time series are shown. No tilt corrections have been made, but tilt angles were small, less than  $3^\circ$ , and the resulting bias in  $w$  is less than  $2.5 \text{ cm s}^{-1}$ .

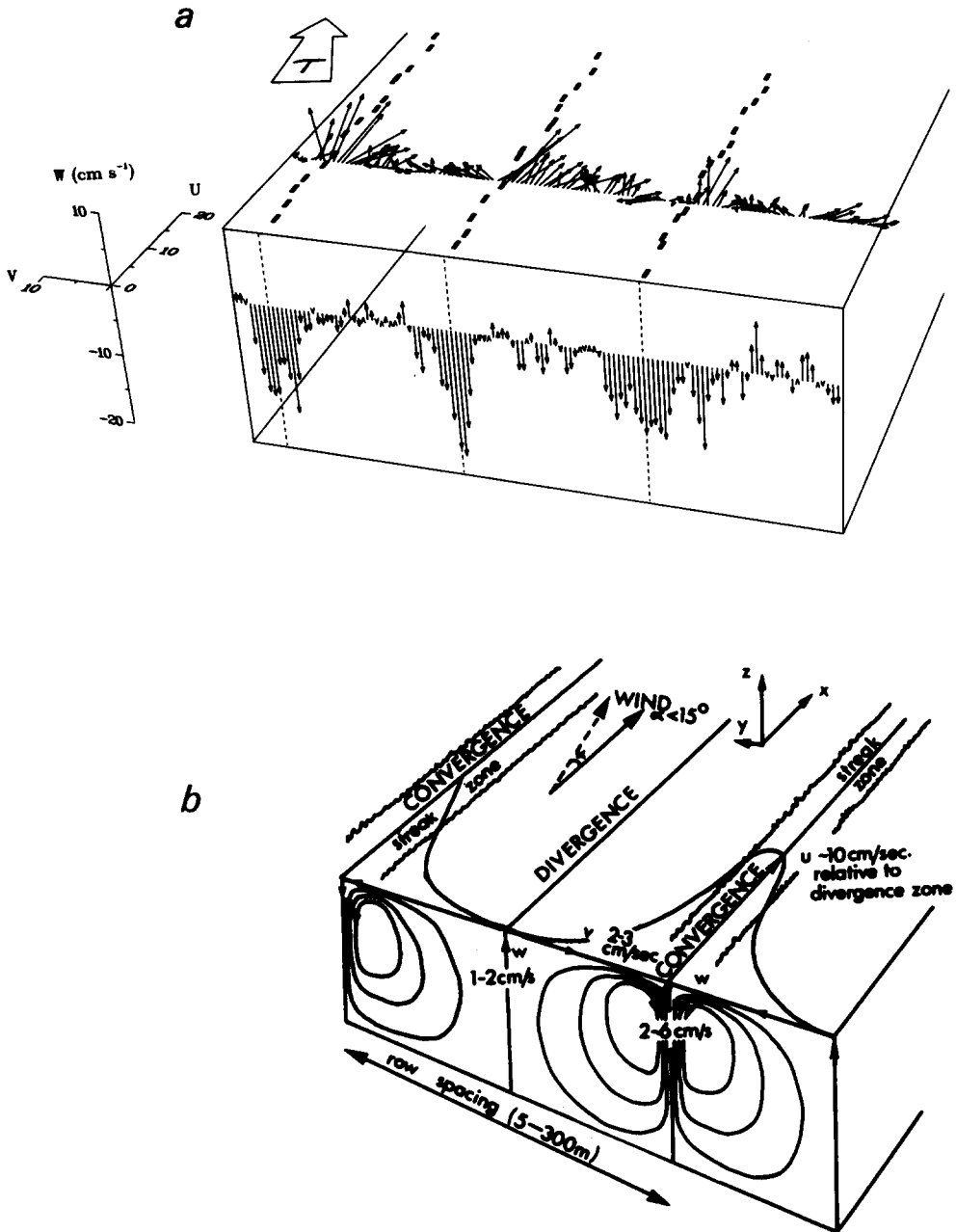


Fig. 8. Comparison of RTP data (a) from the December 1982 cruise (as shown in WELLER *et al.*, 1985) with POLLARD's (1977) visualization (b) of Langmuir circulation. In (a) 30 min of data from the RTP are shown that were collected with the instrument parked at a depth of 23 m. Vertical velocity data subjected to a 3 point running mean are shown on the forward face of the figure, and horizontal velocity data from the same depth (23 m) are shown on the top surface. The downwelling and downwind velocity signals were encountered by the RTP in convergence regions marked by computer cards.

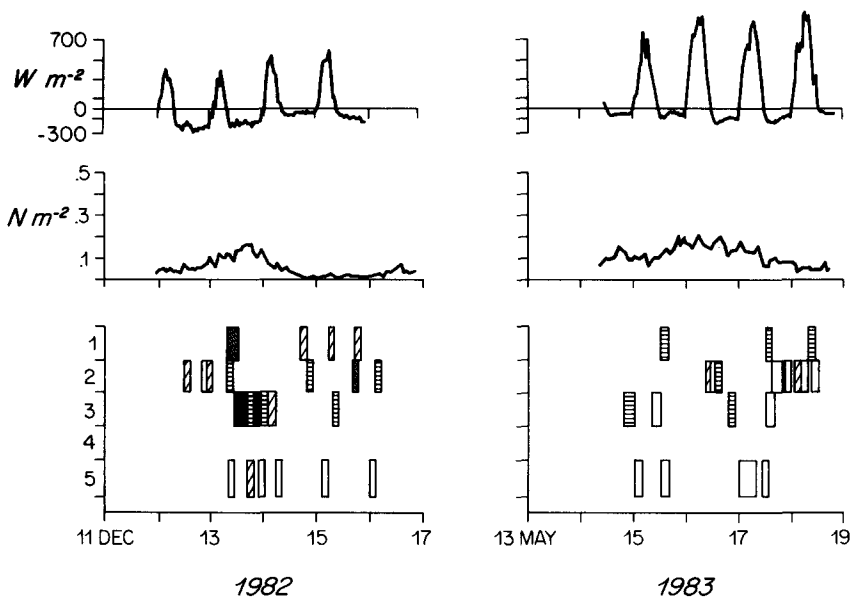


Fig. 9. The net heat flux, the wind stress, and the occurrence and strength of Langmuir circulation during the December 1982 and May 1983 cruises. For Figs 9 and 10 the intensity of the Langmuir circulation is summarized as a function of time (horizontally) and depth (vertically) by the shading inside the boxes. The boxes indicate periods of observation at that depth; level 1 is the surface, 2 is 0–15 m, 3 is 15–30 m, 4 is the fixed depth of 20 m, and 5 is 30 m to the base of the mixed layer. No shading inside a box indicates that observations were made but no Langmuir circulation was observed. For level 1 surface drifter observations were quantized by the length of time needed for the initial scattered distribution of cards to form into organized lines; black indicates alignment within 1–2 min, closely spaced slanted lines indicate alignment took up to 10 min, horizontal lines indicate alignment took 30–60 min, and the most widely spaced lines indicate alignment required more than 1 h. For RTP observations at the various depths indicated by levels 2, 3, 4, and 5 the same shading scale is used, with the shades (darkest first) corresponding to downwelling speeds  $>25 \text{ cm s}^{-1}$ ,  $15\text{--}25 \text{ cm s}^{-1}$ ,  $5\text{--}15 \text{ cm s}^{-1}$ , and  $<5 \text{ cm s}^{-1}$  but  $>0$ .

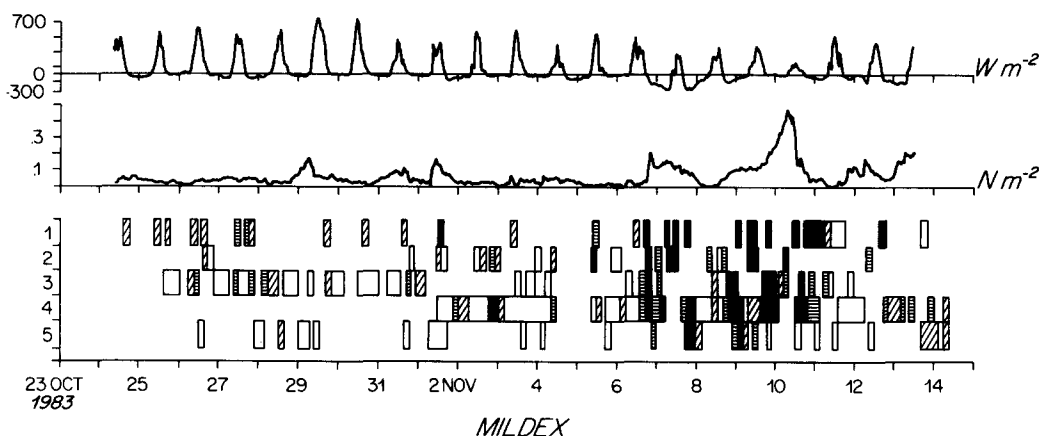


Fig. 10. The net heat flux, the wind stress, and the occurrence and strength of Langmuir circulation during MILDEX. The density of the shading has the same meaning as that given in the caption to Fig. 9. In MILDEX a second RTP was deployed at the fixed depth of 20 m, providing data for level 4 except when being serviced or being moved to permit servicing of other instruments.

larger than the  $2\text{--}3\text{ cm s}^{-1}$  bias possible due to tilt. The upward going vertical velocity had less range, reaching a maximum of  $7\text{--}8\text{ cm s}^{-1}$ , but was often close to the RTP's limit of accurate detection,  $2\text{ cm s}^{-1}$ . Upward flow was also less event-like, and thus more difficult to monitor. As a result our analysis of the temporal variability, depth of penetration and other characteristics of Langmuir circulation focuses on the downwelling signal.

In December 1982 the strongest downwelling was observed during the strongest wind. In May 1983, though the winds were the same strength as the strongest winds of December 1982, weaker downwelling was observed that did not penetrate deeply into the mixed layer. During MILDEX, in the summer-like conditions of the first part of the cruise, the Langmuir circulation was weak to moderate, with maximum downwelling speeds of  $5\text{--}10\text{ cm s}^{-1}$ , and tended to be found fairly near the surface. An increase in wind velocity on 1 November produced strong surface convergence and near-surface downwelling that did not penetrate beyond 15 m into the weakly stratified mixed layer. Late on 6 November until early on 8 November the wind was stronger and moderate Langmuir circulation was observed throughout the mixed layer. The strongest flows were observed as the wind forcing changed direction and increased on 8 and 9 November. The leveling off of the wind early on 10 November was accompanied by an immediate decrease at mid-depth of the strength of the downwelling. As the wind shifted direction and decreased in strength on 10 and 11 November, slightly stronger downwelling was observed.

The data displayed in Figs 9 and 10 show a general correlation between the downwelling speed,  $w$ , and the wind speed but do not support a simple linear relation. Downwelling flows of greater than  $3\text{ cm s}^{-1}$  were observed at wind speeds down to approximately  $1.5\text{ m s}^{-1}$ . Below that wind speed, no significant downwelling was found with the RTP. Figure 11 shows that while the maximum observed  $w$  generally increased with increasing wind speed, a wide range of smaller  $w$  values were also observed at any

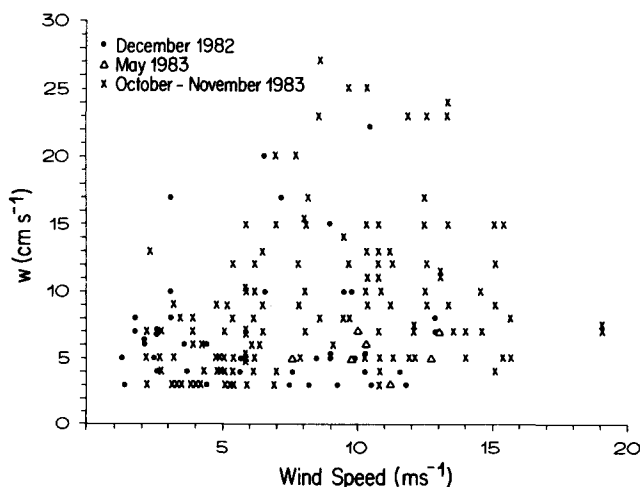


Fig. 11. The observations of downwelling speed,  $w$ , obtained with the RTP plotted against wind speed. Data are taken from all three cruises and from various depths within the mixed layer. Downwelling speeds below  $3\text{ cm s}^{-1}$  were not plotted.

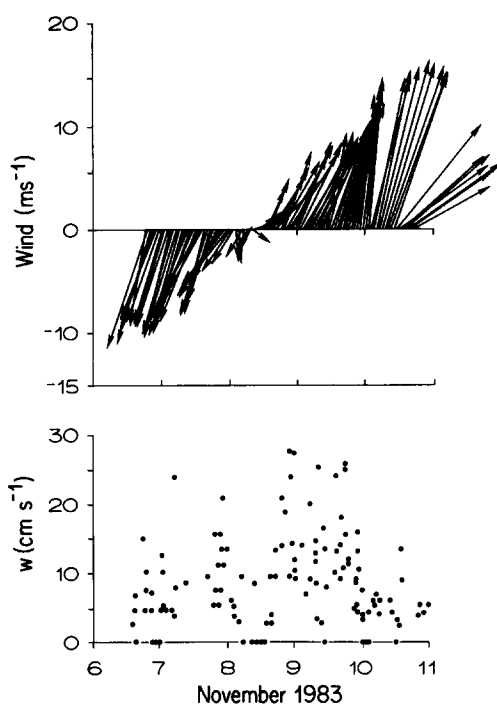


Fig. 12. Hourly averaged wind velocity and downwelling speeds for 6–11 November 1983. A value of 0 for  $w$  indicates that the RTP was in the water at that time and did not observe downwelling. During this time the RTP occupied various depths; all the  $w$  data from the various depths have been plotted.

given wind speed. The variability observed on 6–11 November (Fig. 12) suggested that other factors, perhaps changes in wind direction as well as speed, also effect the size of  $w$ .

One likely reason for the great range of downwelling speeds observed over relatively short time intervals is the presence of a multiplicity of scales of Langmuir cells. The surface drifters showed this particularly well. On many occasions, the cards initially formed into short lines several meters in length, separated by several meters. These lines were then carried into longer lines, up to tens of meters in length and 10–40 m apart. When *Flip* stayed within sight of these lines, further coalescence was sometimes observed, with all the cards forming into only one or two long lines separated by an estimated 100 m. Such large scales match the size of the Langmuir cells detected by the Doppler sonar; SMITH *et al.* (1987) found convergence zones 1–2 km in length, separated by a distance of approximately three times the mixed layer depth. However, if at any time new cards were scattered, they again revealed the presence of the small, several meter wide cells, and the slow migration of the card lines from small spacings to large would be repeated. Thus, a hierarchy of scales of convergent flow patterns existed. It was not easy to detect and identify unambiguously the velocity signals associated with the smaller, presumably weaker cells. Thus, some of the results in this discussion are probably biased toward the larger, stronger cells. However, a multiplicity of scales and a corresponding range of downwelling speeds were likely present and probably contributed to the scatter in Figs 11 and 12.

The RTP also showed a crosswind maximum in the downwind horizontal velocities in the region of convergent, downwelling flow. The signal was largest at the depth of the maximum downward velocity, where it was comparable in size to the downwelling, indicating that the flow there penetrated the mixed layer at an angle of approximately 45°. In contrast, profiles of horizontal velocity in the mixed layer away from the downwelling regions had much less vertical shear.

#### *Data from the VMCMs*

Because of the relatively large size of the downwind velocity in convergent regions and because of the low rate of advection of the Langmuir cells past *Flip*, the horizontal velocities in individual downwelling regions of the Langmuir cells could, at times, be observed by the VMCMs suspended from *Flip*'s booms. However, because the VMCMs vector-averaged horizontal velocities over 1 min intervals, these observations of Langmuir cells may be biased even further than the preceding discussion of the RTP data toward stronger, larger cells and toward times when the drift rate of such features past *Flip* was small. During the December 1982 cruise both strong, large scale and weaker near-surface Langmuir cells were observed. The downwind flow associated with the stronger features was observed by the VMCM located at a fixed depth of 2 m and by the VMCM that profiled between approximately 5 and 65 m. As *Flip* drifted, encountering surface convergences that could be marked by computer cards, the 2 m VMCM data showed a series of downwind anomalies, and the vertical profiles varied from slab-like profiles showing little vertical shear, collected from regions away from and between lines of computer cards, to profiles with a downwind jet, collected in and near a line of computer cards. During the May 1983 cruise, weak to moderate Langmuir cell activity was observed with the RTP. Profiling VMCM data again showed evidence of the subsurface downwind jet embedded in the mixed layer in the convergence zone between adjacent Langmuir cells.

The analysis of the VMCM data from MILDEX, where a combination of profiling and fixed depth instruments provided good resolution of the horizontal velocity field, focused on determining the characteristics of the downwind flow associated with Langmuir cells, especially its magnitude and vertical structure. Examples of the temporal variation in the vertical structure of the horizontal velocity in the mixed layer as Langmuir cells advected past are shown in Figs 13 and 14. When the intensity of the Langmuir circulation was moderate and when the southerly wind was dying late on 7 November to early on 8 November, the maximum of the downwind flow (Fig. 13) approached  $30 \text{ cm s}^{-1}$ . After the wind had reversed on November 9 the most energetic Langmuir circulation was observed and the downwind maximum (Fig. 14) was over  $40 \text{ cm s}^{-1}$ .

The vertical shear of horizontal velocity associated with the downwind jet was estimated both by differencing successive velocity values in a profile and by subtracting time series of horizontal velocity at one depth from that at another depth. Figure 15 shows the profile of shear in the convergence zone based on horizontal velocity profile number 183 made during 9 November. Time series of shear near the surface, computed using the 2 and 6.5 m VMCMs (Fig. 16), shows a quasi-regular modulation in shear, which was at times large, with  $\Delta U/\Delta z \approx 25 \text{ cm s}^{-1}/4.5 \text{ m} = 5.6 \times 10^{-2} \text{ s}^{-1}$ . The contribution of the Langmuir circulation to the mixed layer shear was, in fact, quite striking. Figure 17 shows daily distributions of 2–6.5 m velocity difference vectors during MILDEX. Days of stronger Langmuir cell activity, as judged by the vertical velocity data

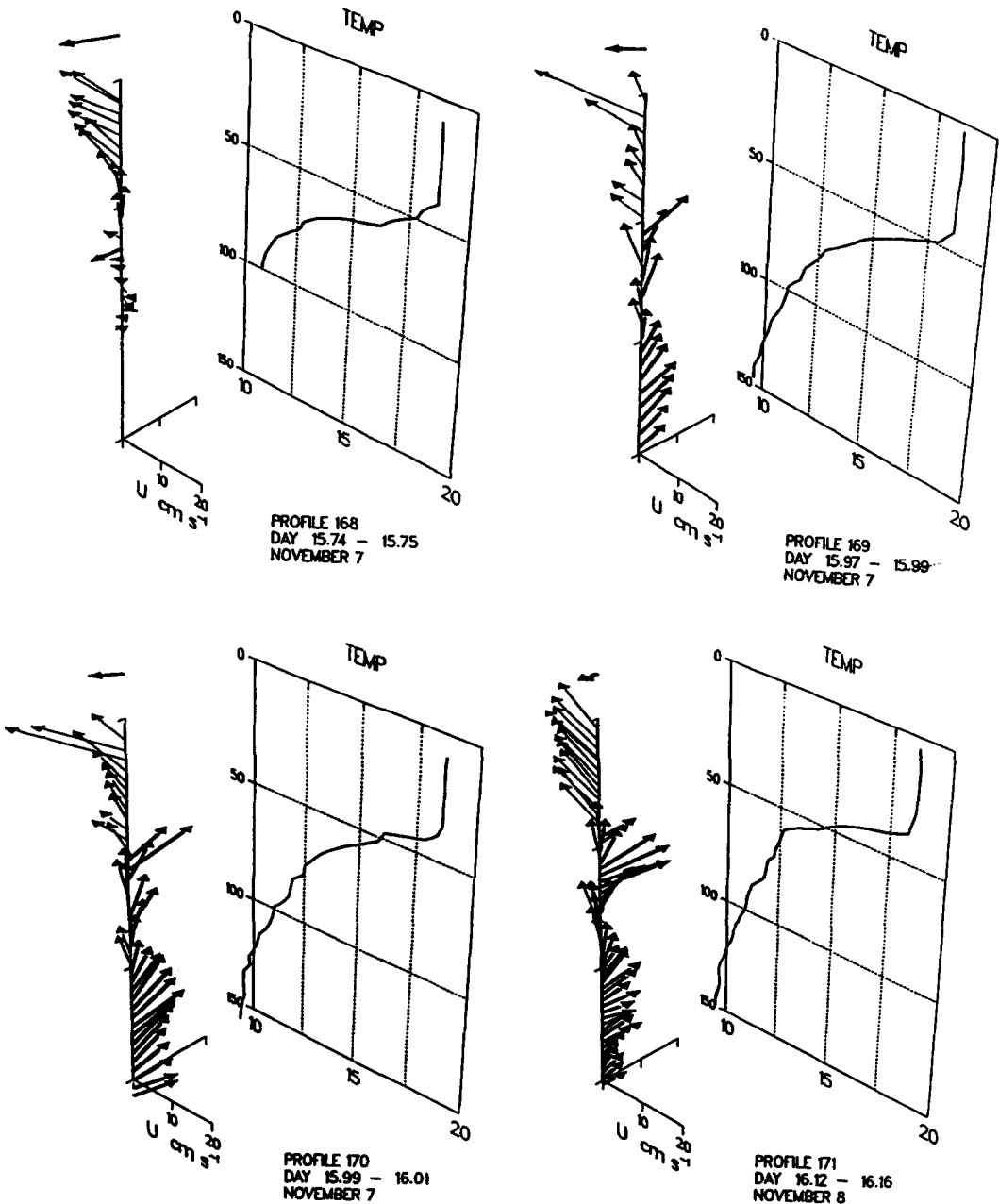


Fig. 13. Vertical profiles of horizontal velocity and temperature obtained by a profiling VMCM. The arrow above the velocity axes indicates the direction and relative strength of the wind at the time of the profile. These are successive profiles from the afternoon of 7 November to the morning of 8 November (local). These velocities are absolute velocities.

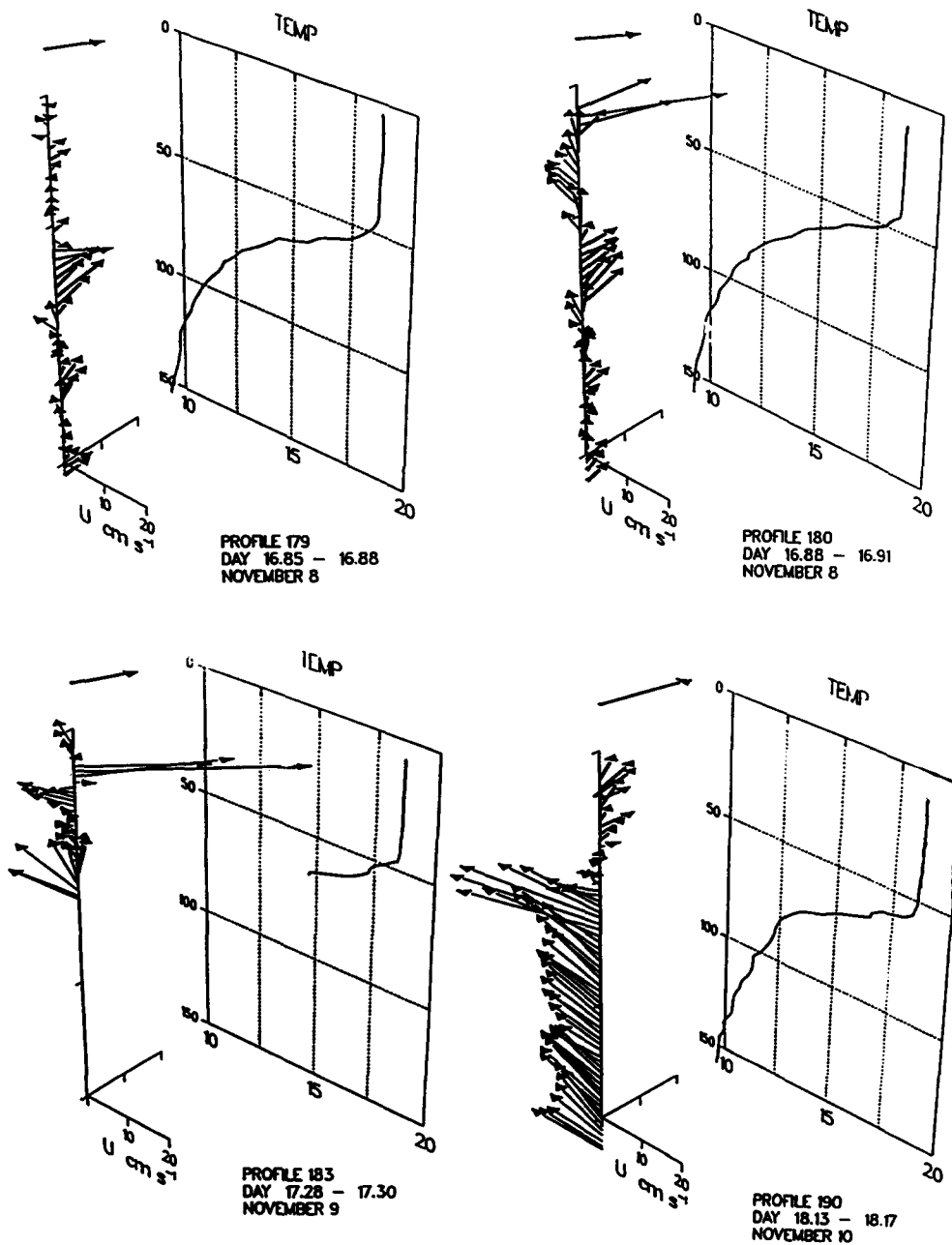


Fig. 14. Vertical profiles of absolute horizontal velocity and temperature obtained by a profiling VMCM on 8-10 November (local). (Profiles 181, 182 and 184-189 did not include data from within the mixed layer.)

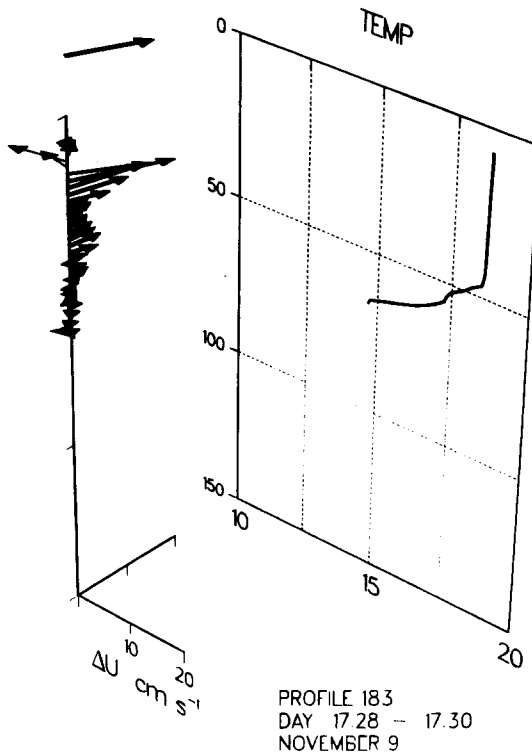


Fig. 15. Data from profile 183 (Fig. 14) were used to create this profile of the vertical shear of horizontal velocity in the downwind jet. The velocities in profile 183 were first differenced, and those velocity difference vectors ( $\text{cm s}^{-1}$ ) are shown here. Note that near the surface, above the maximum in the downwind flow, the shear is directed upwind. Wind direction is indicated, as in Figs 13 and 14, by the arrow above the velocity axes.

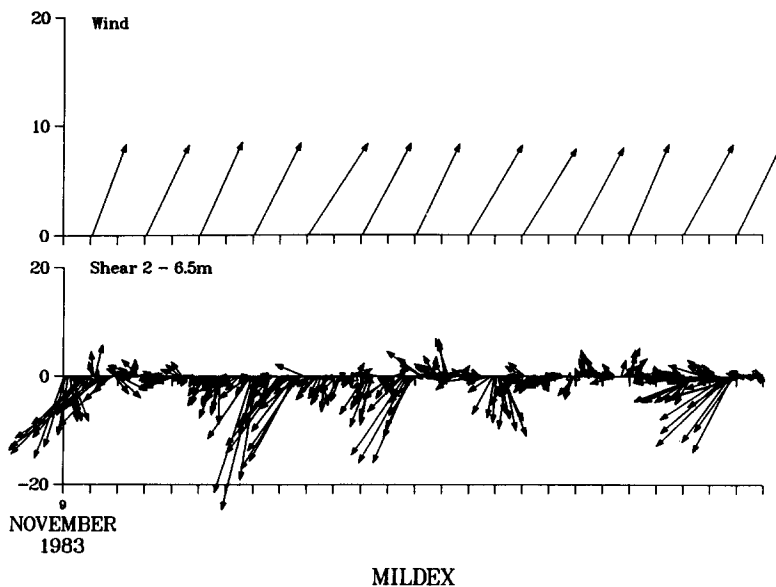


Fig. 16. Time series of the wind velocity and the near-surface shear. The vector difference,  $(U(2 \text{ m}) - U(6.5 \text{ m}))$ , is plotted, one vector per minute, for the first part of 9 November. Thirty-min averaged wind velocity vectors are shown, and the time ticks are 10 min apart.

(Fig. 10), were days when a significant fraction of the velocity difference vectors pointed upwind (i.e. they were approximately  $180^\circ$  out of phase with the wind, indicating that downwind flow was greater at 6.5 m) with a bias for the left, upwind quadrant, because the downwind jets were most often directed slightly toward the right of the wind. Below the depth of the downwind velocity maximum, the velocity difference vector reversed direction, and velocity differences,  $(U(20\text{ m}) - U(35\text{ m}))$ , available only after 3 November, showed a downwind bias on the days that the 2–6.5 m shear was biased upwind (Fig. 18). Similar plots for the 6.5–20 m shear showed both downwind (third

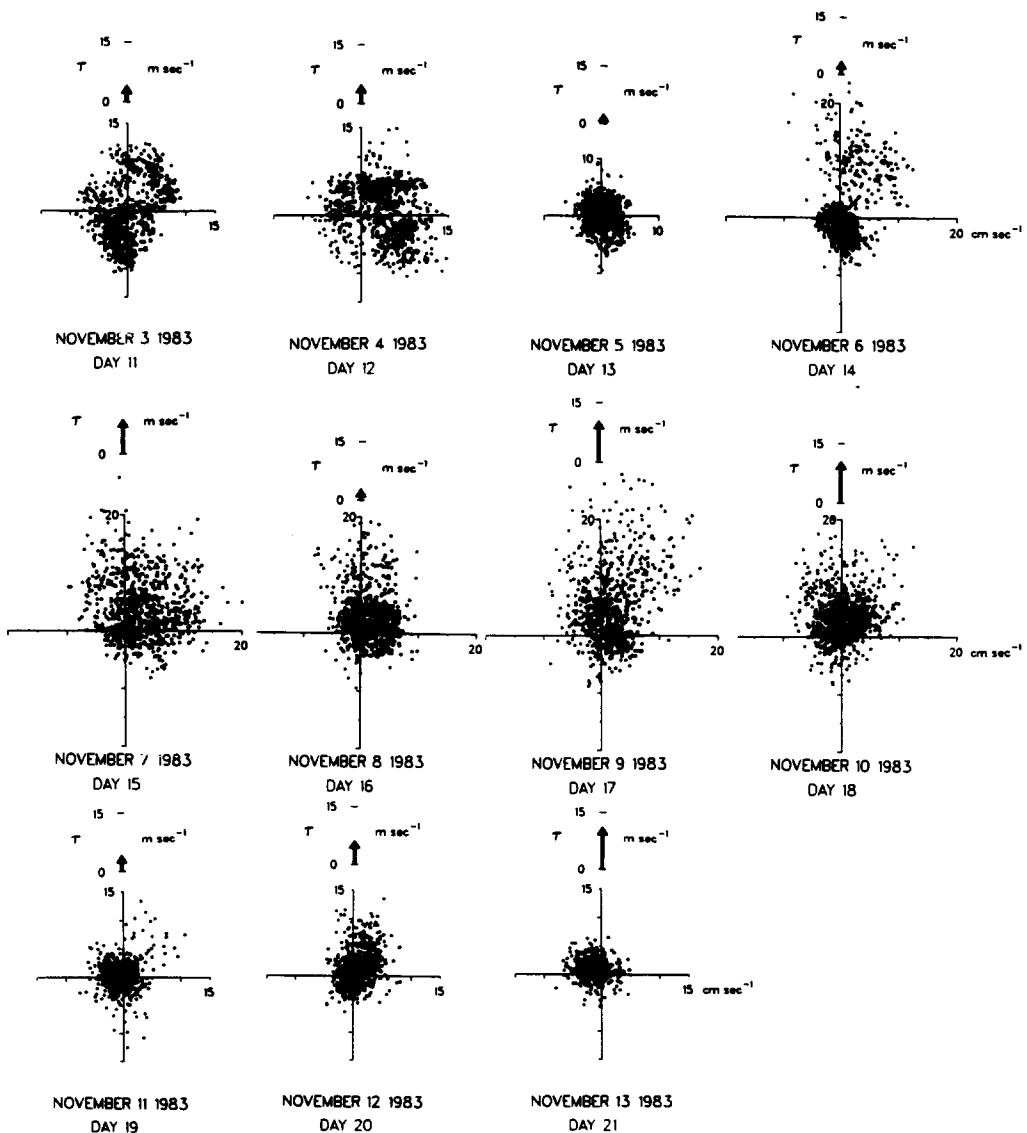


Fig. 18. Daily summaries of the vector  $(U(20\text{ m}) - U(35\text{ m}))$ . Data from these depths were available from 3 November onward and have been treated as in Fig. 17.

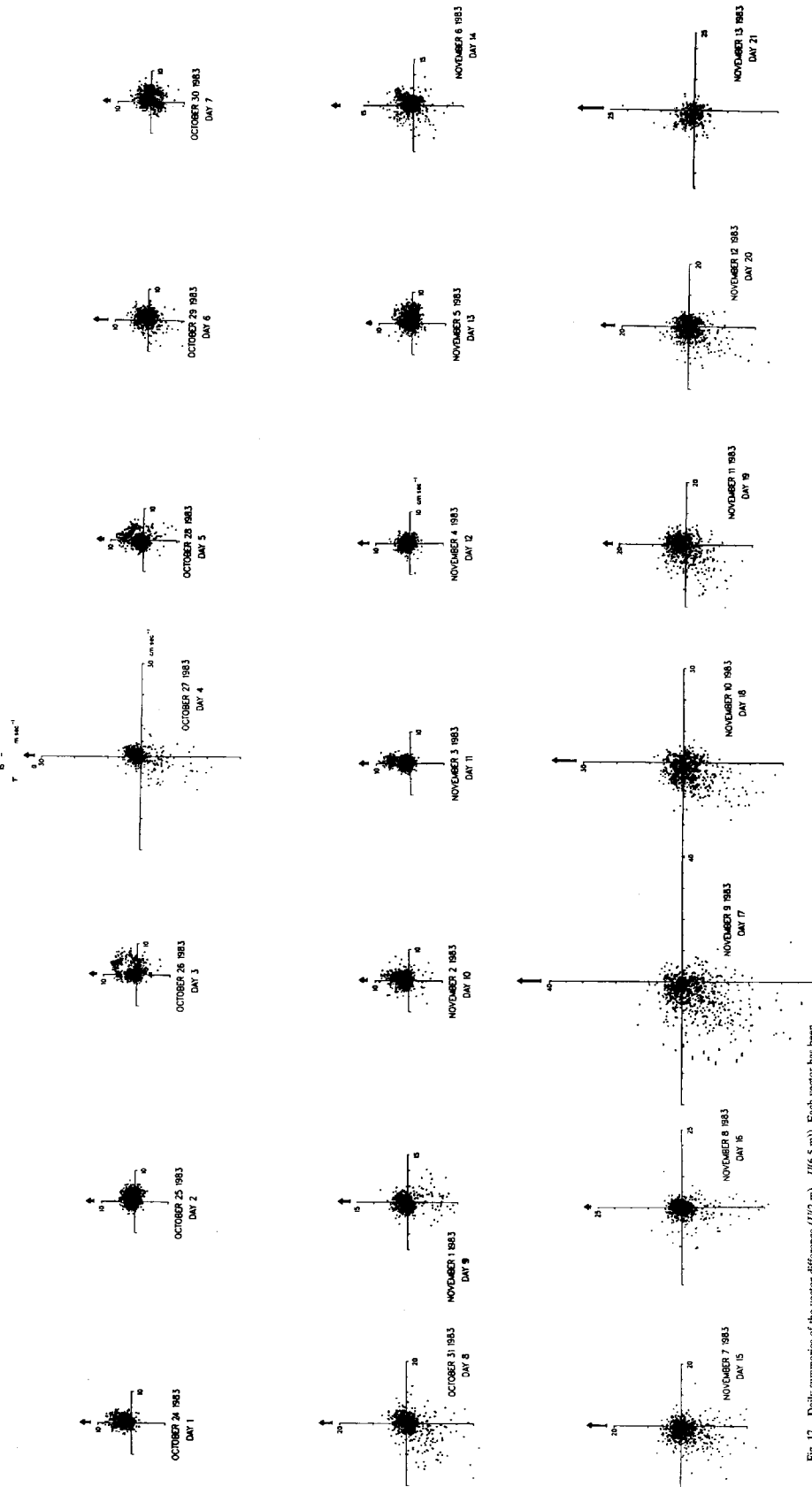


Fig. 17. Daily summaries of the vector difference  $(U(2\text{ m}) - U(6.5\text{ m}))$ . Each vector has been rotated, together with the coincident wind velocity vector, so that the wind points along the vertical axis of the plot. The horizontal axis is the magnitude of the wind velocity vector. A dot was placed to indicate the location of the head of each velocity difference vector. The length of the broad vertical arrow at the top of each plot is proportional to the magnitude of the daily-averaged wind velocity; the scale for the wind is shown on the plot for 27 October.

quadrant, minus  $u$  and minus  $v$ ) and upwind (first quadrant, plus  $u$  and plus  $v$ ) velocity difference vectors on days of strong Langmuir circulation; apparently the depth of the downwind maxima associated with various individual cells varied between 6.5 and 20 m during these days. Time series of velocity differences at greater depths (30–50 m, 50–65 m) failed to show a shear signal that could be correlated with that observed near the surface (2–6.5 m) in the Langmuir cells.

In the frequency domain, the Langmuir cells contributed to near-surface shear in a frequency band bounded roughly by 2 and 10 cph. The bounds of this frequency band depended on the rate of advection (approximately  $5\text{--}15\text{ cm s}^{-1}$ ) of cells past *Flip* and on the spacing (up to approximately 150 m) of the large cells that had measurable downwind flow. Spectra of shear (Fig. 19) indicate increased energy content in this band down to depths of 35 m; below that depth the shear was dominated by lower frequency variability. Band-passing the shear time series in a broad band of 1–14 cph to capture the variability associated with Langmuir circulation produced a record of its temporal and vertical variability (Fig. 20) analogous to that developed using the vertical velocity data (Fig. 10). The shear time series, like the vertical velocity data (e.g. Fig. 12), showed that the intensity of Langmuir circulation did not always track the magnitude of the wind speed. For example, late on 27 October and early on 1 November 1983, Langmuir cells appeared as the wind stress direction (rather than its magnitude) changed; and late on 9 November the intensity of the shear and strength of the downwelling decreased even as the magnitude of the wind stress increased.

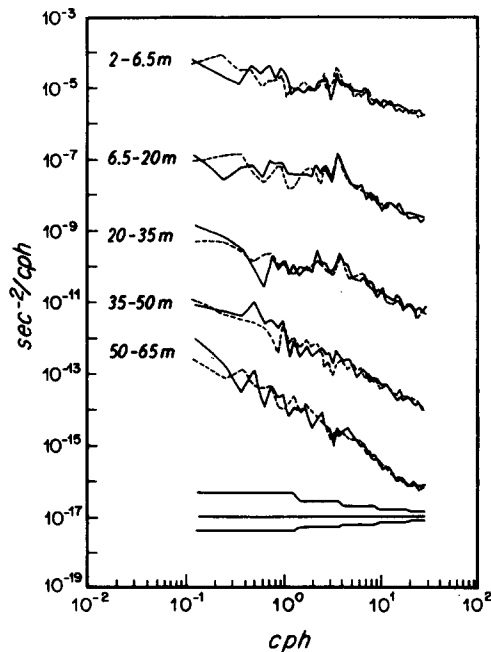
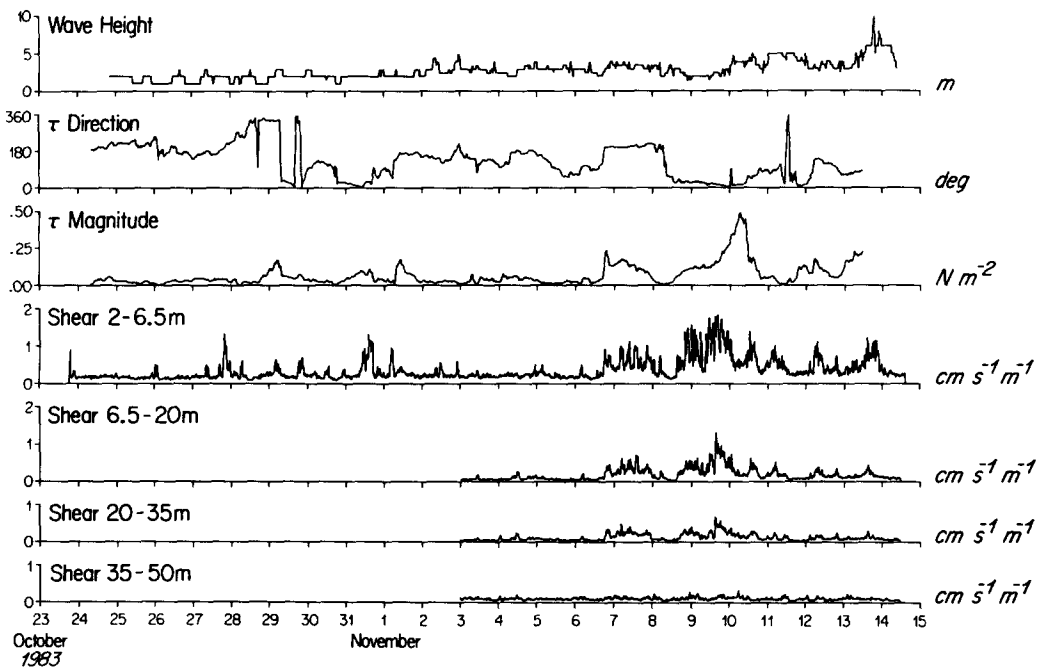


Fig. 19. Rotary autospectra of the vertical shear of horizontal velocity for 9 November 1983 from five depth pairs, 2–6.5, 6.5–20, 20–35, 35–50, and 50–65 m. The top spectrum is at the proper location relative to the vertical axis; each spectrum below is shifted down an additional two decades. The solid line is the clockwise spectrum; the dashed line is the counter-clockwise spectrum. The 95% confidence limits are indicated.



### MILDEX

Fig. 20. Time series of wave height (eyeball observation), direction of the wind stress (direction toward), magnitude of the wind stress, and magnitude of the shear in the 2-14 cph band at depth pairs 2-6.5, 6.5-20, 20-35, and 25-50 m.

#### 4. THE EFFECT OF LANGMUIR CIRCULATION ON THE STRUCTURE OF THE MIXED LAYER

Incoming solar radiation is absorbed near the surface and, when the wind mixing is weak, restratification can result in the upper 10-15 m, as shown in Fig. 6. Mixing of the upper part of this restratified fluid can then result in a shallow mixed layer superimposed on the deeper, relict, mixed layer. This shallow mixed layer, because it is associated with diurnal heating, is often called the diurnal mixed layer. The Langmuir circulation observed from *Flip* was at times strong, capable of carrying fluid on a circuit from the sea surface to the interior of the mixed layer and back in minutes. Such strong three-dimensional flow should, if it appeared suddenly, rapidly reduce near-surface vertical gradients associated with the air-sea fluxes. As well, once established, strong Langmuir circulation should then maintain the homogeneity of the mixed layer. In an attempt to determine the effect of Langmuir circulation on the structure of the mixed layer, these hypotheses were tested by examining the interaction of the three-dimensional flow with the diurnal cycle of near-surface temperature structure and by noting if the mean vertical shear of horizontal velocity and/or the stratification within the mixed layer was reduced on days characterized by the presence of strong Langmuir cells.

During the December 1982 cruise, when the winds were light on 14-15 December, sea surface temperatures increased and vertical temperature structure was found near the

surface at midday. Comparison of the unaveraged time series of sea surface temperature (SST) and the temperature at 2 m showed not only the general trend of midday warming but also the occurrence of brief negative dips in SST with coincident positive spikes in the 2 m temperature record. Both anomalies were approximately  $0.5^{\circ}\text{C}$  in size. The horizontal velocity data from the VMCM at 2 m showed downwind flow anomalies at the same time as these temperature fluctuations and suggested a link between the temperature events and the shallow, moderate Langmuir cells then present.

Failure of the SST sensor in May prevented use of data from the second cruise to examine the interaction of Langmuir circulation and the temperature structure of the diurnal mixed layer, but such interaction was readily apparent in the MILDEX data. On 25–26 October 1983, for example (Fig. 21), air–sea heat flux led to surface heating and restratification in the late morning, and low frequency near-surface velocity shear grew as temperature difference grew. The shear vector initially accelerated downwind and then rotated to the right of the wind as reported in PRICE *et al.* (1986). In the late afternoon, under reduced heating, the temperature difference began to decrease. At about 2100 on 25 October, this decrease greatly accelerated and the temperature gradient abruptly disappeared. Coincident with that, Langmuir cells were observed as evidenced by periodic, upwind events in the shear vector. Figure 21 shows 3-min averaged velocity

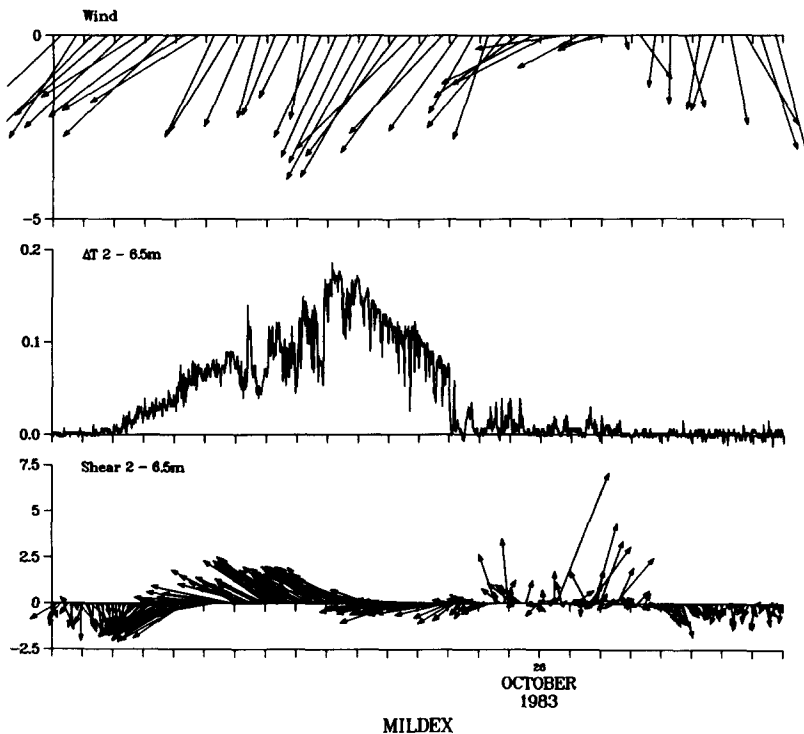


Fig. 21. Time series of 30-min averaged wind velocity (top,  $\text{m s}^{-1}$ ), temperature difference (2–6.5 m, middle,  $^{\circ}\text{C}$ ), and 3-min averaged velocity difference (2–6.5 m, bottom,  $\text{cm s}^{-1}$ ) for parts of 25–26 October 1983. The time ticks are hourly, time is local, and the plot starts at 0800 on 25 October.

difference vectors for clarity, and this averaging makes the suddenness of the appearance of the Langmuir cells less apparent at 2100 than in the raw data.

Examination of the raw data from MILDEX showed that weak or intermittent Langmuir cells, when present in the stratified part of the diurnal mixed layer, produced, as observed in December 1982, negative temperature anomalies at the surface and positive anomalies at 2 m. However, the appearance of a field of Langmuir cells of moderate size (horizontal scales in excess of 10 m) and strength (downwelling greater than  $5 \text{ cm s}^{-1}$ ) or of larger, stronger cells was quickly followed by complete mixing of the near-surface stratification as observed late on 25 October.

Events such as that shown in Fig. 21 required certain conditions, the existence of the stratification and the sudden appearance of Langmuir circulation, and were observed but several times during MILDEX, typically late in the afternoon. When the mixed layer was without significant stratification, temperature signals associated with the cells were small and considerably more difficult to detect. Positive anomalies, typically  $0.005\text{--}0.015^\circ\text{C}$  in magnitude, were found in the downwelling flow in the convergent regions during daytime heating; and negative anomalies of similar size were found during night-time cooling (WELLER *et al.*, 1985). The small size and change in sign of the anomaly with the change in sign of the surface heat flux suggested that moderate to strong Langmuir cells rapidly swept surface and near-surface water into the convergence regions and then down into the interior of the mixed layer.

A general picture of the variability in the structure of the mixed layer was developed by examining the coincident distribution of near-surface stratification and shear during MILDEX, which was summarized by daily plots of  $\alpha g \Delta z$  ( $\alpha$  is the coefficient of thermal expansion) times the temperature difference,  $\Delta T(2\text{--}6.5 \text{ m})$ , against velocity difference,  $\Delta U(2\text{--}6.5 \text{ m})$ , squared (Fig. 22). The ratio of the first quantity to the second is an approximate finite difference form of the non-dimensional Richardson number,  $R_i$ . On days of weak Langmuir circulation, 24–25 and 30 October and 3 November, near-surface temperature and velocity gradients coexisted, and the majority of the data points fall near and above the  $R_i = 0.25$  line. On plots for other days, 26–30 October and 2, 4–6, 11 and 14 November, two groups of data points are present; one group fills in near the  $R_i = 1$  line and the other along the velocity difference squared axis. The plots for the third group of days, 31 October and 1, 7–10, 12 and 13 November, are dominated by points along the shear axis; stratification was small, but shear was large, as large as  $37 \text{ cm s}^{-1}/4.5 \text{ m} = 8 \times 10^{-2} \text{ s}^{-1}$  (9 November). The large shears in the absence of stratification can be traced to the presence of the downwind jets found in the convergence zones between adjacent Langmuir cells. Thus, Fig. 22 suggests a dominance by Langmuir circulation of the near-surface temperature and velocity structure of the ocean on certain days (the third group); on such days little or no diurnal signal was seen in SST (Fig. 5). A short-lived appearance of Langmuir circulation on other days (the second group) temporarily homogenized the near-surface temperature field, such as late on 25 October and early the next day (Fig. 21), but stratified shear flow was otherwise present. During the first group of days, the weak Langmuir circulation either did not penetrate to the 2–6.5 m depth range or was incapable of mixing the mean stratification at that depth.

Variability in the vertical shear of horizontal velocity linked to Langmuir circulation was apparent (Fig. 20) down to 20–35 m depths. At these depths, as near the surface, the presence of strong Langmuir circulations was associated with greatly reduced stratification. However, below the 20–35 m depth range, Langmuir circulation did not have a

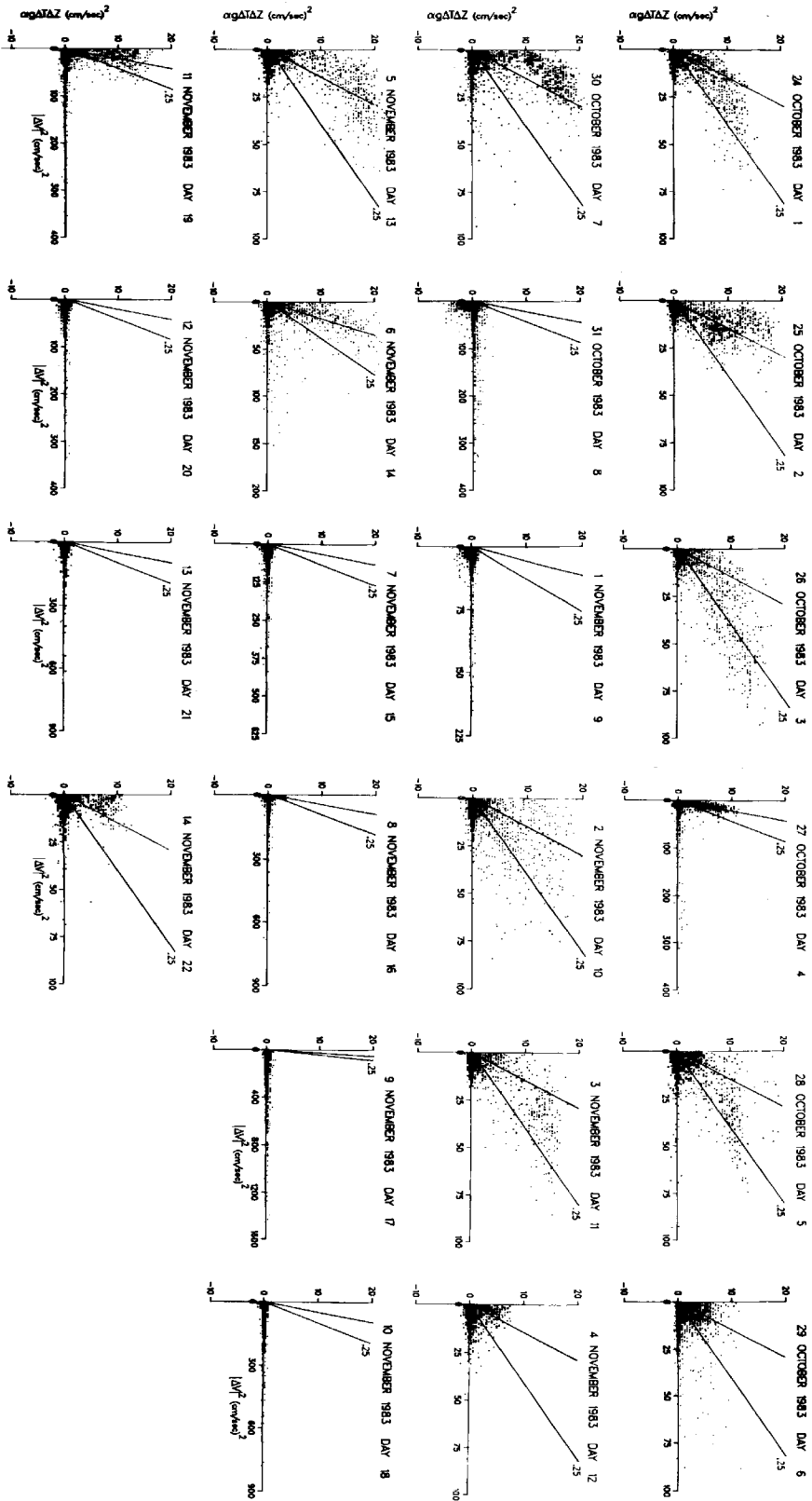


Fig. 22. Daily summaries of the joint distribution of velocity and temperature differences ( $2-6.5$  m) as the coefficient of thermal expansion. The scale of the velocity axis is varied to cover the observed range of shear; for reference, lines of slope 1 and 0.25 are plotted.

discernable effect on the structure of the mixed layer. As the base of the mixed layer was approached, little shear variability was found in the 1–14 cph band; instead, shear at inertial and lower periods became more energetic. Similarly, at these depths, there was no apparent link between changes in stratification and Langmuir cell activity observed nearer the surface. Stratification persisted, for example, in the 35–50 m region to 9 November, the time of the most intense Langmuir cells. Only somewhat later, on 10–13 November, was the stratification in this region reduced as the mixed layer deepened. Once the stratification decreased so did the shear; and it appears that the mixing and mixed layer deepening were associated with low frequency shear across the base of the mixed layer rather than with Langmuir circulation.

The near-surface water carried down into the interior of the mixed layer by the convergent and then downwelling flow of the Langmuir cells was accelerated by the wind stress as well as heated (or cooled) by the air–sea heat flux. In addition to reducing near-surface temperature gradients, it was anticipated that the mean wind-driven, near-surface, shear would also be absent or greatly reduced when strong Langmuir circulation was present. Daily averages of the 1 min vector velocity difference time series (each vector rotated so that the simultaneous wind vector pointed north, as discussed in Section 3) were computed (Table 1). Surprisingly, based on the velocity differences in Table 1, daily-averaged velocity hodographs for 31 October and 1, 7–13 November showed a subsurface maximum in mean horizontal velocity. In fact, all of the third group

Table 1. Daily-averaged values of wind speed and vector velocity differences computed using VMCM data from 2, 6.5, 20, 35 and 50 m. Data at the three deepest depths were available only after 2 November. The original 1 m velocity vectors were rotated so that the wind vector at that time pointed north; positive V is thus the downwind direction

Day	Wind speed (m s <sup>-1</sup> )	$\Delta U, \Delta V$ (cm s <sup>-1</sup> )							
		(2–6.5)		(6.5–20)		(20–35)		(35–50)	
October									
24	4.9	0.39,	2.43						
25	3.6	0.90,	0.83						
26	3.3	0.93,	1.27						
27	4.9	0.05,	0.75						
28	3.2	-0.34,	1.40						
29	6.5	0.69,	0.53						
30	3.2	0.84,	0.54						
31	6.1	-0.40,	-0.92						
November									
1	5.4	-0.44,	0.26						
2	3.8	0.13,	1.70						
3	4.2	0.08,	1.85	1.55,	-0.53	-0.12,	-0.31	-0.38,	0.63
4	4.9	0.09,	0.74	3.81,	3.60	3.19,	0.71	-0.59,	-1.33
5	2.6	0.98,	0.69	0.30,	-0.14	0.03,	0.32	2.34,	1.10
6	3.6	0.28,	1.35	1.14,	-0.13	0.89,	0.98	-1.51,	3.70
7	8.9	-1.91,	-0.48	-1.45,	-1.10	2.51,	3.87	2.53,	-4.67
8	3.1	-0.50,	-0.62	0.91,	-0.25	1.36,	2.77	0.76,	-1.86
9	10.5	-3.73,	-2.87	2.04,	0.48	1.59,	4.91	-0.98,	-1.83
10	10.7	-2.49,	-1.43	1.81,	2.41	-0.08,	3.34	5.26,	-1.05
11	4.3	-1.09,	0.76	0.77,	1.56	-0.73,	0.45	-1.52,	-0.12
12	6.4	-1.00,	-0.29	0.87,	1.77	0.71,	1.20	0.18,	1.65
13	11.3	-1.73,	0.75	0.10,	1.94	-1.42,	0.83	2.83,	4.46

of days, those in which near-surface structure was dominated by Langmuir cells, and one of the second group (11 November), those in which strong cells were present part of the day, were characterized by a subsurface maximum in the mean horizontal velocity.

The mean velocity differences on these days are considered to be significant when larger than  $1 \text{ cm s}^{-1}$  in amplitude. Improper sampling of the surface wave field should be minimized by deploying the instruments from *Flip*; such errors, like Stokes drift, would contribute to downwind shear rather than upwind shear. Underestimation of the mean flow is possible with a VMCM (WELLER and DAVIS, 1980), but is reported to be small, at worst, 6%, in the surface wave field (BEARDSLEY, 1987). On a day such as 9 November, the downwind flow in the convergence zones at 6.5 m was larger (far in excess of 6%) than that at 2 m, and the downwind flow elsewhere was nearly independent of depth. Thus, after averaging across many cells, the mean downwind flow at 6.5 m was indeed larger than that at 2 m, so that the mean shear was upwind between 2 and 6.5 m at approximately  $0.01 \text{ s}^{-1}$ . This suggests that the vertical transport of horizontal momentum by the Langmuir cells has a dependence on depth in the mixed layer that is higher order in  $z$  than linear.

These results and the characteristics of the Langmuir circulation observed from *Flip* are discussed further in the context of other published results in the next section.

## 5. COMPARISON WITH PREVIOUS OBSERVATIONS

Many of the previous observations of Langmuir circulation had been made at or very near the surface, and the characteristics deduced from such observations are somewhat different than those presented here. It is worthwhile, then, to point out briefly some of the differences and also the similarities between the earlier results and those presented here.

### *Magnitude of the downwelling*

Vertical velocity measurements by LANGMUIR (1938) and later by SUTCLIFFE *et al.* (1963) and others were made with horizontal plates attached to buoyant vertical poles (Sutcliffe floats). LEIBOVICH (1983) summarized many of the data with two linear relations,  $w \propto 8.5 \times 10^{-3} U_w$  and  $w \propto 2.5 \times 10^{-3} U_w$ , where  $w$ , the downwelling speed, and  $U_w$ , the wind speed, are both in  $\text{cm s}^{-1}$ . FILATOV *et al.* (1981) made Sutcliffe float measurements in Lake Ladoga, Russia and suggested a parameterization for  $w$  of the form  $w = aU_w^b$ , where  $a$  and  $b$  depended on the air-sea temperature difference;  $a = 3.6 \times 10^{-2}$  and  $b = 0.7$  for  $T_{\text{AIR}}$  equal to the sea surface temperature (SST),  $a = 3.7 \times 10^{-2}$  and  $b = 0.7$  for  $T_{\text{AIR}}$  greater than SST, and  $a = 1.6 \times 10^{-2}$  and  $b = 0.6$  for  $T_{\text{AIR}}$  less than SST, where  $w$  and  $U_w$  are in  $\text{cm s}^{-1}$ . Our measurements showed that downwelling velocity increased away from the surface and was strongest, for the largest scale cells, at between 6 and 20 m when the mixed layer was between 40 and 60 m deep. Thus, Sutcliffe float measurements made very near the surface underestimated the maximum downwelling speed to be found in the mixed layer. Figure 23 shows that the RTP vertical velocities are, at a given wind speed, greater than or equal to those given by the FILATOV *et al.* (1981) formulae and also often greater than the values suggested by the two equations given by LEIBOVICH (1983).

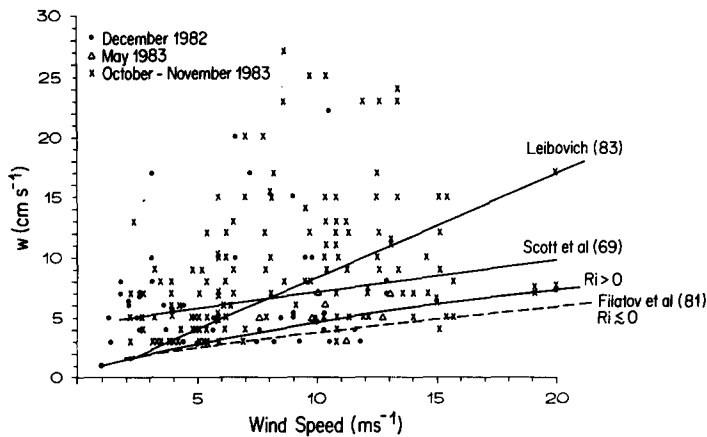


Fig. 23. Comparison of the dependence of vertical velocity on wind speed suggested by LEIBOVICH (1983) [to the data of HARRIS and LOTT (1973) and SUTCLIFFE *et al.* (1963)], by SCOTT *et al.* (1969), and by FILATOV *et al.* (1981) with the vertical velocity data collected by the RTP from *Flip*.

#### *Functional dependence of $w$ on wind speed and wave height*

LEIBOVICH (1983) and others cite  $3 \text{ m s}^{-1}$  as a minimum wind speed for Langmuir circulation to appear. KENNEY (1977) noted that beginning at wind speeds of approximately  $3 \text{ m s}^{-1}$ , wave breaking and other processes produce foam that existing Langmuir cells organize into visible lines on the surface and suggested that past observers had incorrectly interpreted this wind speed as a minimum required for Langmuir circulation. Downwelling was observed from *Flip* at wind speeds down to  $1.5 \text{ m s}^{-1}$ , and no support was found for an absolute minimum wind speed required for cell formation. FALLER'S (1981) reanalysis of data collected by STOMMEL (1952) in ponds on Cape Cod presented a similar conclusion; surface windrows were observed on the ponds at wind speeds well below  $3 \text{ m s}^{-1}$ .

The goodness of fit of the Sutcliffe float data to a linear relation between  $w$  and  $U_w$  was cited by LEIBOVICH (1983) as support for the proportionality of  $w$  to  $U_w$ . The *Flip* data support a general trend of increasing  $w$  values with higher winds. Some of the scatter in Fig. 23 is associated with the RTP data being drawn from various depths in the mixed layer, but even sorting the data by depth bins does not reduce the scatter to the point where the data are well fit by a straight line. Further, the data also provide exceptions to such a simple parameterization (Fig. 11). Present theories of Langmuir circulation involve the surface waves. Interaction between the waves and perturbations in the downwind flow field provide the driving or vortex force term in LEIBOVICH'S (1977) equations. Thus, a dependence of the intensity of the Langmuir circulation on sea state as well as wind speed might be anticipated. The wave height time series from MILDEX, however, did not add sufficient information to explain the observed variation in the intensity of the Langmuir cells (Fig. 24). For example, a decrease in the intensity of the three-dimensional flow began late on 9 November and continued through the beginning of 10 November, while both wind speed and wave height were growing. However LEIBOVICH'S (1977) non-dimensional equations include a non-dimensional grouping called the Langmuir number,  $La = (\nu_T^3 k^2 / \sigma a^2 u_*^2)^{1/2}$ , where  $\nu_T$  is an eddy viscosity,  $u_*$  is the friction

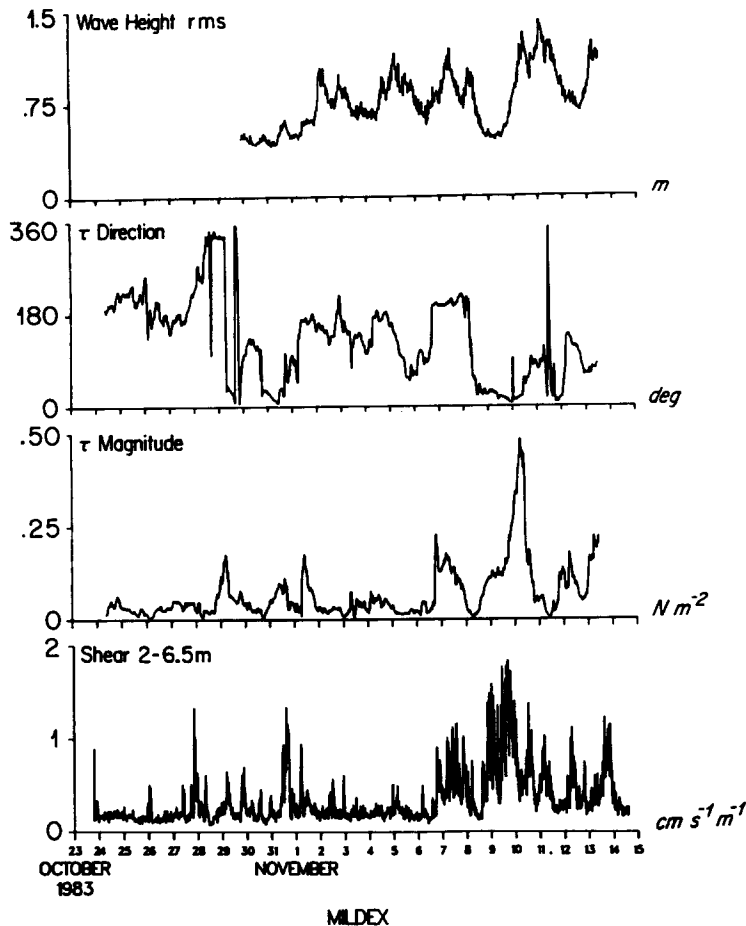


Fig. 24. Time series (top to bottom) of wave height, wind stress direction, wind stress magnitude, and band-passed (2–14 cph) shear (2–6.5 m).

velocity, and  $a$ ,  $\sigma$ , and  $k$  are wave height, wave frequency, and wavenumber, respectively; and demonstration of the dependence of Langmuir circulation on surface wave conditions may require a more complete surface wave data set than that collected in MILDEX.

#### *Langmuir cells and near-surface temperature structure*

THORPE and HALL (1982) cite McLEISH's (1968) observations of cold streaks aligned with the wind and also McLEISH's (1970) reports of slicks with temperatures  $0.23^{\circ}\text{C}$  cooler than outside the slick. WANNAMAKER's (1980) shipboard survey, made under calm conditions and by steaming across slicks, had also showed similar, strong, near-surface temperature anomalies, approximately  $1\text{--}1.5^{\circ}\text{C}$  negative excursions at  $0.05\text{ m}$  and coincident positive spikes of the same size at  $4\text{ m}$  depth. Under stronger wind and wave conditions THORPE and HALL (1982) found evidence for a temperature anomaly beneath the slicks that was small and positive (about  $0.008^{\circ}\text{C}$ ) at the surface and extended

down and slightly to the left of the wind beneath the slick. Both such temperature anomalies were observed on *Flip*. In calm conditions SST and 2 m temperature time series showed large (approximately 0.5°C) anomalies when shallow Langmuir cells interacted with the stratification of a shallow diurnal mixed layer without mixing it away. Under stronger winds, Langmuir cells observed from *Flip* mixed the near-surface stratification, had larger scales, greater penetration, and much smaller temperature anomalies (0.005–0.015°C), similar to those reported by THORPE and HALL (1982).

#### *Vertical penetration*

SCOTT *et al.* (1969) used an instrumented surface float to make observations of near-surface temperature structure found in conjunction with surface slicks and concluded that Langmuir circulation penetrated only until the first significant thermocline. FILATOV *et al.* (1981) reported observations from Lake Ladoga that showed the depth of penetration of the Langmuir circulation to be proportional to wind speed and also inversely proportional to stratification; however, in the Lake Ladoga experiments, penetration was limited by the shallow bottom. The *Flip* observations showed the Langmuir circulation to be biased toward the top half of the oceanic mixed layer. Evidence of either downwelling or horizontal flow associated with Langmuir cells that penetrated to the base of the relict mixed layer was not found. The flow near the base of the relict mixed layer associated with the cells may have been too weak to be detected by the RTP or VMCMs, or it may have been stopped by diurnal temperature gradients encountered above the base of the relict mixed layer.

#### *Horizontal scales*

The surface drifters deployed from *Flip* often indicated that a variety of horizontal scales coexisted but provided little new quantitative information about those scales. The presence of many different scales of Langmuir cells has been observed by many previous surface drifter experiments. McLEISH (1968), for example, reported that sulfur dust distributed by a crop dusting plane at first formed irregular lines, with many intersections and relatively small scales, and later formed into longer, nearly parallel lines with larger separation. SCOTT *et al.* (1969) reported that streak spacing correlated with the depth of the first significant stable layer, but not with wind speed or surface heat loss. RYANZHIN (1982) reported sharply defined primary convergence bands and also weaker, closer together secondary bands in Lake Ladoga, and expressed both a primary and a secondary crosswind scale as linear functions of wind speed. In experiments in the shallow Lake of the Woods (KENNEY, 1977) the largest scale was set by the water depth. The maximum spacing of the Langmuir cells, observed from *Flip* with the Doppler sonar (SMITH *et al.*, 1987), was approximately three times the depth of the mixed layer and, on 9–11 November, maintained that scaling as the mixed layer depth varied slowly due to internal tides. This result suggests that mixed layer depth determines the maximum horizontal scale and is consistent with laboratory results (FALLER and CAPONI, 1978), where the ratio of cell width to water depth was between 2.5 and 3.5.

#### *Horizontal velocity*

Observations in Lake Ladoga with current meters measuring horizontal velocities (RYANZHIN, 1983) showed a peak in the spectrum of horizontal velocity between 0.025 and 0.045 rad s<sup>-1</sup> (characteristic time scales of  $2\pi/\text{freq} = 2\text{--}6$  min and frequencies of

10–30 cph) associated with the Langmuir circulation. With increasing wind speed the signal became more energetic and the lower frequency limit of the spectral peak associated with the Langmuir circulation shifted lower. The *Flip* current meter observations recorded similar variability in horizontal velocity as the Langmuir cells were advected past. The peak in the horizontal velocity spectra was less pronounced than that noted by RYANZHIN (1983), but Langmuir circulation observed from *Flip* was at times transient and also was not dominated by a single horizontal scale size as it is in shallow lakes.

Subsurface maxima in either the downwind flow in the convergence regions or in the mean downwind flow have not, apparently, been reported in discussions of previous field studies. Vertical profiles of the mean downwind flow associated with Langmuir circulation based on time-dependent numerical solutions (LEIBOVICH, 1977) showed a surface maximum, a local minimum just below, and then an increase to a smaller, subsurface maximum. In a later study (LEIBOVICH and PAOLUCCI, 1980) the subsurface maximum in the mean current profiles was less pronounced and occurred at a depth below the depth of the maximum downwelling. Downwelling again had a subsurface maximum, but the profiles of the instantaneous horizontal velocity in the convergence regions lacked the distinct subsurface downwind maximum observed from *Flip*.

#### SUMMARY AND DISCUSSION

The primary conclusions of the field studies of three-dimensional flow within the mixed layer conducted from the R.P. *Flip* are:

(1) Cellular flow patterns were often observed that matched the characteristics of Langmuir circulation. On the surface, drift cards were drawn into lines that formed approximately parallel to the surface wind. Beneath the surface convergences, downward vertical flow and downwind horizontal flow were observed. Measurements of the flow in the convergence zones found that the horizontal component was directed slightly off to the right of the wind.

(2) The downward vertical velocities observed by the Real Time Profiler (RTP) were larger (up to  $27 \text{ cm s}^{-1}$ ) than those previously reported. The RTP data showed the maximum vertical velocity to be located below the surface and above mid-depth in the mixed layer. We suspect that previous measurements made at or near the surface have underestimated the maximum downwelling speed.

(3) The downwind flow in the convergence regions also had a subsurface maximum, so that near the surface the vertical shear of horizontal velocity in the convergence zones was directed upwind. The horizontal velocity in the jet was of the same order of magnitude as the vertical velocity, so that flow in the convergence regions was directed downward at an angle of approximately  $45^\circ$ . Daily averages of horizontal velocity showed that the mean profile of horizontal velocity could have a subsurface maximum when Langmuir cells were a dominant feature of the near-surface flow field.

(4) Langmuir cells were found to be highly transient. These observations were insufficient to determine the conditions required for either their appearance and growth, or for their decay. Counter-examples were observed to the notion that downwelling speed is proportional to wind speed.

(5) When Langmuir cells appeared, they were able to rapidly mix away the near-surface stratification associated with weak, shallow diurnal mixed layers (stratification

approximately  $\leq 0.05^\circ\text{C m}^{-1}$ ). From this we conclude that Langmuir circulation can be an important direct mixing mechanism in the upper one third to one half of the mixed layer. However, we found no evidence that Langmuir cells play a direct role in mixing near the base of the 40–60 m deep mixed layer observed during these experiments.

The description of Langmuir circulation given here is far from complete, and further study of Langmuir circulation is needed. The geometry of the Langmuir cells needs further exploration. As the Langmuir cells were advected past *Flip*, vertical profiling VMCMs and RTPs and VMCMs held at fixed depths resolved only limited portions of the three-dimensional flow, essentially only the downwind, downwelling jets. Resolution and detailed spatial sampling of other parts of the three-dimensional flow were lacking. Thus, it is not possible, for example, to accurately calculate the average Reynolds stress,  $\langle uw \rangle$ , where  $u$  is the downwind component, associated with a field of Langmuir cells. Very strong downwind, downward flows were observed, but were transient. The strong correlation of the downwind and downward components of velocity in the Langmuir cells has been noted by POLLARD (1977), GORDON (1970) and others. GORDON (1970) suggested that Langmuir circulation with an upwelling of on average  $1.5 \text{ cm s}^{-1}$ , a maximum downwelling of  $4 \text{ cm s}^{-1}$ , and an excess downwind flow in the convergence zone of approximately  $2 \text{ cm s}^{-1}$  would have an associated Reynolds stress an order of magnitude larger than that available from the observed wind ( $5 \text{ m s}^{-1}$ ). The *Flip* observations confirmed the strong correlation, and also showed that the magnitudes of the maximum downwelling and downwind flows could be much higher than GORDON'S (1970) estimates. However, due to the lack of resolution of the detailed spatial structure of the Langmuir cells, we were unable to arrive at estimates of the vertical transfer of horizontal momentum and other properties that were any significant improvement in accuracy over those of GORDON (1970) and POLLARD (1977). It is clear, however, that higher velocities observed from *Flip* lend even more support to the conclusion that the apparent Reynolds stress associated with the Langmuir cells is far in excess of that available from the wind stress alone.

Previous conceptualizations of the three-dimensional flow pattern associated with Langmuir cells, such as that produced by POLLARD (1977) (Fig. 8), and results from numerical models have shown streamlines coming together into a region of downwelling narrowly confined in the crosswind direction. The streamlines in the downwelling flow then remain parallel for a significant fraction of the vertical extent of the cell. One implication of this pattern is that the downwelling, downwind flow has a maximum that is rather broad in vertical extent, though narrow in the crosswind direction. The *Flip* measurements, however, suggest that the subsurface maxima in both the downwelling and downwind components of the flow are narrowly confined in the vertical as well as in the crosswind direction.

The downwind flow associated with Langmuir cells deserves general consideration in future mixed layer studies. From a practical point of view, the presence of large vertical shears in the convergence regions will complicate attempts to use Lagrangian drifters to sample the near-surface velocity and shear fields. In terms of mixed layer dynamics, considerable variability in both horizontal velocity and vertical shear is added to the mixed layer when Langmuir cells are present. LEIBOVICH and PAOLUCCI (1980) pointed out that shear-flow instability and mixing may arise due to vertical gradients in the downwind flow; the shear actually observed from *Flip* is much larger than that in their model profiles, and it would be interesting to investigate variations in the level of mixed

layer turbulence associated with Langmuir circulation. The downwind velocity signal does not average to zero across many cells, so there can be a subsurface maximum in the mean horizontal velocity field. At this point, however, the contribution of Langmuir circulation to the mean flow in the mixed layer has not been quantified. Nor has the dependence of the growth of Langmuir circulation on near-surface shear, either the Lagrangian shear associated with surface waves or mean Eulerian shear, been determined. In further analysis of the MILDEX data an attempt will be made to contrast the wind-driven response when Langmuir cells are absent with that observed when they were present and, if possible, to separate the downwind flow associated with the Langmuir cells from the wind-driven, Ekman flow.

*Acknowledgements*—This work was funded by the Office of Naval Research, Contract N00014-84-C-0134, NR 083-400. Jerry Dean provided the ability to measure vertical velocities by designing and building the Real Time Profiler. The onboard data acquisition and real time display hardware and software system associated with the Real Time Profiler was put together by Erika Francis. Nancy Pennington and Chris Light assisted in processing the data and in the preparation of this manuscript. Discussions with colleagues, including Alan Fallor and Henry Stommel, and manuscripts of work in progress supplied by Steve Thorpe helped convince us to attempt the direct measurement of the vertical velocities; and their encouragement is gratefully acknowledged. The Buoy Group at Woods Hole Oceanographic Institution provided support for the field work as well as the Vector Measuring Current Meters and Vector Averaging Wind Recorder. The work on *Flip* was made possible, in a large part, by the excellent cooperation and support of the Marine Physical Laboratory of the Scripps Institution of Oceanography, especially Rob Pinkel and Eric Slater, and by the skills and good will of DeWitt Efrid and the rest of the crew of the R.P. *Flip*. The editor and the reviewers are thanked for comments that led to improvements in the manuscript. Contribution 6493 from The Woods Hole Oceanographic Institution.

#### REFERENCES

- BEARDSLEY R. C. (1987) A comparison of the VACM and the new EG&G VMCM on a surface mooring in CODE-1. *Journal of Geophysical Research*, **92**, 1845–1859.
- FALLER A. J. (1981) The origin and development of laboratory models and analogues of the ocean. In: *Evolution of physical oceanography. Scientific surveys in honor of Henry Stommel*, B. A. WARREN and C. WUNSCH, editors, MIT Press, Cambridge, pp. 462–480.
- FALLER A. J. and E. A. CAPONI (1978) Laboratory studies of wind-driven Langmuir circulations. *Journal of Geophysical Research*, **83**, 3617–3633.
- FALLER A. J. and C. PERINI (1983) The role of Langmuir circulations in gas transfer across natural water surfaces. Technical note BN-1000, Institute for Physical Science and Technology, University of Maryland, College Park, 10 pp.
- FALLER A. J. and S. J. AUER (1987) The roles of Langmuir circulations in the dispersion of surface tracers. Technical note BN-1058, Institute for Physical Science and Technology, University of Maryland, College Park, 60 pp.
- FILATOV N. N., S. V. RYANZHIN and L. V. ZAYCEV (1981) Investigation of turbulence and Langmuir circulation in Lake Ladoga. *Great Lakes Research*, **7**, 1–6.
- GORDON A. L. (1970) Vertical momentum flux accomplished by Langmuir circulation. *Journal of Geophysical Research*, **75**, 4177–4179.
- HARRIS G. P. and J. N. A. LOTT (1973) Observations of Langmuir circulations in Lake Ontario. *Limnology and Oceanography*, **18**, 584–589.
- KENNEY B. C. (1977) An experimental investigation of the fluctuating currents responsible for the generation of windrows. Ph.D. Thesis, University of Waterloo, 163 pp.
- LANGMUIR I. (1938) Surface motion of water induced by wind. *Science*, **87**, 119–123.
- LEIBOVICH S. (1977) On the evolution of the system of wind drift currents and Langmuir circulations in the ocean. Part 1. Theory and averaged current. *Journal of Fluid Mechanics*, **9**, 715–743.
- LEIBOVICH S. (1983) The form and dynamics of Langmuir circulations. *Annual Review of Fluid Mechanics*, **15**, 391–427.
- LEIBOVICH S. and S. PAOLUCCI (1980) The Langmuir circulation instability as a mixing mechanism in the upper ocean. *Journal of Physical Oceanography*, **10**, 186–207.
- MCLEISH W. (1968) On the mechanism of wind-slick generation. *Deep-Sea Research*, **15**, 461–469.
- MCLEISH W. (1970) Spatial spectra of ocean surface temperature. *Journal of Geophysical Research*, **75**, 6872–6877.

- POLLARD R. T. (1977) Observations and theories of Langmuir circulations and their role in near surface mixing. In: *A Voyage of Discovery: G. Deacon 70th Anniversary Volume*, M. ANGEL, editor, Pergamon Press, New York, pp. 235–251.
- PRICE J. F., R. A. WELLER and R. PINKEL (1986) Diurnal cycling: Observations and models of the upper ocean response to diurnal heating, cooling, and wind-mixing. *Journal of Geophysical Research*, **91**, 8411–8427.
- RYANZHIN S. V. (1982) Transverse dimensions of Langmuir circulation cells in a lake in the absence of a thermocline. *Izvestiya, Atmospheric and Oceanic Physics*, **18**, 814–820.
- RYANZHIN S. V. (1983) The kinematics of horizontal flows in circulating Langmuir cells. *Izvestiya, Atmospheric and Oceanic Physics*, **19**, 41–46.
- SCOTT J. T., G. E. MEYER, R. STEWART and E. G. WALTHER (1969) On the mechanism of Langmuir circulations and their role in epilimnion mixing. *Limnology and Oceanography*, **14**, 493–503.
- SMITH J., R. PINKEL and R. WELLER (1987) Velocity structure in the mixed layer during MILDEX. *Journal of Physical Oceanography*, **17**, 425–439.
- STOMMEL H. (1952) Streaks of natural water surfaces. In: *International Symposium on Atmospheric Turbulence in the Boundary Layer*, E. W. HEWSON, editor, *Geophysical Research Papers* No. 19, Air Force Cambridge Research Center, Cambridge, Massachusetts, pp. 145–154.
- SUNDBY S. (1983) A one-dimensional model for the vertical distribution of pelagic fish eggs in the mixed layer. *Deep-Sea Research*, **30**, 645–661.
- SUTCLIFFE W. H., Jr, E. R. BAYLOR and D. W. MENZEL (1983) Sea surface chemistry and Langmuir circulation. *Deep-Sea Research*, **10**, 233–243.
- THORPE S. A. and A. J. HALL (1982) Observations of the thermal structure of Langmuir circulation. *Journal of Fluid Mechanics*, **114**, 237–250.
- WANNAMAKER B. (1980) Surface slicks and near-surface variability: A literature review and some measurements in the Gulf of Cadiz. *SACLANTCEN Memorandum SM-133*, La Spezia, Italy, 10 pp.
- WELLER R. A. (1978) Observations of horizontal velocity in the upper ocean made with a new vector measuring current meter, Ph.D. Thesis, Scripps Institution of Oceanography, University of California, San Diego, 169 pp.
- WELLER R. A. (1981) Observations of the velocity response to wind forcing in the upper ocean. *Journal of Geophysical Research*, **86**, 1969–1977.
- WELLER R. A. and R. E. DAVIS (1980) A vector-measuring current meter. *Deep-Sea Research*, **27**, 562–582.
- WELLER R. A., J. P. DEAN, J. MARRA, J. F. PRICE, E. A. FRANCIS and D. C. BOARDMAN (1985) Three-dimensional flow in the upper ocean. *Science*, **227**, 1552–1556.